

AFFDL-TR-77-79, Vol. III

Flaw Growth in Complex Structure Volume III Summary, Assessments, Conclusions

Lockheed-California Company
A Division of Lockheed Corporation
Burbank, California 91520

December 1977

Final Report

12 May 1975 - 12 September 1977

Distribution Statement

Approved for public release; distribution unlimited.

Prepared for

Air Force Flight Dynamics Laboratory
Air Force Systems Command
Wright-Patterson AFB, Ohio 45433

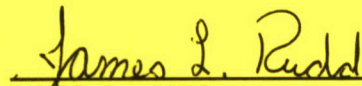
20070924240


NOTICE

When Government drawings, specifications, or other data are used for any purpose other than in connection with a definitely related Government procurement operation, the United States Government thereby incurs no responsibility nor any obligation whatsoever; and the fact that the government may have formulated, furnished, or in any way supplied the said drawings, specifications, or other data, is not to be regarded by implication or otherwise as in any manner licensing the holder or any other person or corporation, or conveying any rights or permission to manufacture, use, or sell any patented invention that may in any way be related thereto.

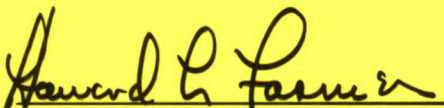
This report has been reviewed by the Information Office (IO) and is releasable to the National Technical Information Service (NTIS). At NTIS, it will be available to the general public, including foreign nations.

This technical report has been reviewed and is approved for publication.


JAMES L. RUDD
Project Engineer


ROBERT M. BADER, Chief
Structural Integrity Branch
Structural Mechanics Division

FOR THE COMMANDER


HOWARD L. FARMER, Colonel, USAF
Chief, Structural Mechanics Division

Copies of this report should not be returned unless return is required by security considerations, contractual obligations, or notice on a specific document.

REPORT DOCUMENTATION PAGE		READ INSTRUCTIONS BEFORE COMPLETING FORM
1. REPORT NUMBER AFFDL-TR-77-79, Vol. III	2. GOVT ACCESSION NO.	3. RECIPIENT'S CATALOG NUMBER
4. TITLE (and Subtitle) FLAW GROWTH IN COMPLEX STRUCTURE FINAL REPORT, VOLUME III SUMMARY, ASSESSMENTS, CONCLUSIONS		5. TYPE OF REPORT Technical - Final PERIOD COVERED May 1975 - September 1977
7. AUTHOR(s) T.R. Brussat and S.T. Chiu, Lockheed-California Company, and M. Creager, Del West Engineering, Chatsworth, California		6. PERFORMING ORG. REPORT NUMBER LR 28272 Vol. III
9. PERFORMING ORGANIZATION NAME AND ADDRESS LOCKHEED-CALIFORNIA COMPANY BURBANK, CALIFORNIA 91520		8. CONTRACT OR GRANT NUMBER(s) F33615-75-C-3093
11. CONTROLLING OFFICE NAME AND ADDRESS Air Force Flight Dynamics Laboratory Air Force Systems Command, (FBE) Wright-Patterson AFB, Ohio 45433		10. PROGRAM ELEMENT, PROJECT, TASK AREA & WORK UNIT NUMBERS 486U-02-09
14. MONITORING AGENCY NAME & ADDRESS (if different from Controlling Office)		12. REPORT DATE December 1977
		13. NUMBER OF PAGES
		15. SECURITY CLASS. (of this report) UNCLASSIFIED
		15a. DECLASSIFICATION/DOWNGRADING SCHEDULE
16. DISTRIBUTION STATEMENT (of this Report)		
17. DISTRIBUTION STATEMENT (of the abstract entered in Block 20, if different from Report)		
18. SUPPLEMENTARY NOTES		
19. KEY WORDS (Continue on reverse side if necessary and identify by block number) Fracture Mechanics, Fatigue, Structure, Testing, Damage Tolerance, Crack Propagation, Analysis, Crack Arrest, Spectrum Loading.		
20. ABSTRACT (Continue on reverse side if necessary and identify by block number) Fatigue crack growth testing and analysis was conducted to evaluate the effects of initial flaw location and multiplicity on fatigue crack growth life and element failure sequence in multiple element, mechanically fastened metallic structure. The test program, including 68 precracked structural specimens consisting of 26 joints and 42 stringer-reinforced panels, is summarized. The test results and corresponding analytical results are presented and compared. With respect to the test results for precracked		

20. ABSTRACT

joints the following effects are discussed: fastener torque, faying surface friction, friction under the fastener head, single and multiple initial flaws, fretting, transverse bending, flush-head and protruding-head fasteners, and spectrum loading effects. With respect to the results for precracked stringer-reinforced panels the following are discussed: longitudinal splice versus continuous skin, initial flaw locations, single or multiple initial flaws, presence of continuing damage flaws, crack growth in a tee or angle stringer, transverse bending, load shedding effects, spectrum loading, fracture surface marking, stress level, and crack path. Guidelines and recommendations based on the results from this program are discussed.

FOREWORD

The experimental and analytical research program reported herein was the responsibility of the Structural Methods Group of the Lockheed-California Company from 12 May 1975 to 12 Sept. 1977. The work was performed for the Air Force Flight Dynamics Laboratory to fulfill the objectives of Contract F33615-75-C3093.

J. L. Rudd was the AFFDL technical monitor, and his continuous interest in every detail was of great technical benefit to the program.

The care that was taken in specimen preparation and testing led to a reliable set of test results. Specimen fabrication and precracking were coordinated by W. P. Renslen with assistance from W. F. Kerwin, both of Del West Engineering. Testing, under the direction of D. E. Pettit, was carried out by the Lockheed Rye Canyon Fatigue Laboratory personnel including F. M. Pickel, D. Black, C. J. Looper, L. Reed, L. Silvas and C. L. Spratt.

Special thanks are in order for W. G. Browne, who provided continuous guidance in budget management and program administration throughout the course of the program. E. K. Walker, J. C. Wordsworth, and J. C. Ekvall are thanked for their valuable contributions in the area of program management as well as their technical consultation. Other in the Stress Department who made significant technical contributions were L. Bakow, W. L. Rakness, P. Schall and R. C. Smith. R. J. Van Ness and the Publication Services Department are appreciated for coordinating the layout, typing and artwork for the final report.

TABLE OF CONTENTS

Section		Page
I	INTRODUCTION AND OBJECTIVES	1
II	SUMMARY OF TESTS	2
1.	PHASE I TESTS	2
2.	PHASE II TESTS	11
III	SUMMARY OF ANALYSIS	14
IV	SUMMARY OF RESULTS	21
1.	PHASE I RESULTS	21
2.	PHASE II RESULTS	40
V	CONCLUSIONS AND RECOMMENDATIONS	52
	REFERENCES	58

LIST OF FIGURES

Figure		Page
1	Summary of Initial Damage Conditions, Double-Lap Shear Specimens	3
2	Summary of Initial Damage Conditions, Single-Lap Shear Specimens	4
3	Summary of Test Results for Continuing Damage Flaws	6
4	Two-Bay Stringer-Reinforced Specimen	8
5	Crack Growth Prediction Method	15
6	Summary of Fatigue Crack Growth Data, 7075-T6 Aluminum, $R = 0.1$, Laboratory Air Environment	16
7	S-N Curve for 3/16 Inch 7075-T6 Aluminum Sheet, $R = 0.1$	17
8	Effects of Continuing Damage Flaws on Life	22
9	Effects of Fastener Type on Total Life	24
10	Effects of Single and Multiple Initial Cracks	26
11	Comparison of Alternate Flaw Locations, Tee-Reinforced Specimens	28
12	Comparison of Alternate Flaw Locations, Edge-Stiffened Specimens	29
13	Specimen for Crack Growth Between Holes (Ref. 2)	31
14	Analytical Crack Growth Predictions, Hole-to-Hole Specimen	32
15	Predicted and Test Lives for Precracked Single-Lap and Double-Lap Joint Specimens	33
16	Comparison of Arrest Times at the Torqued, Interference-Fit Fastener in the Precrack Path	35
17	Summary of Crack Growth Lives for Edge-Stringer Reinforced Specimens	39
18	Baseline Spectrum Crack Growth Rates for the 80-Flight Loading Sequence	41

LIST OF FIGURES (Continued)

Figure		Page
19	Baseline Spectrum Crack Initiation Lives for the 80-Flight Loading Sequence	42
20	Effect of Fastener Head Type in Constant Amplitude Tests of the Single-Lap Joint Specimen	45
21a	Spectrum Test Lives and Life Predictions for Joints	47
21b	Spectrum Test Lives and Life Predictions for Tee-Reinforced Split-Skin Specimens	47
22	Stress Level Effect, Two-Bay Specimen with Precracked Edge Stringer and Skin	49

LIST OF TABLES

Table		Page
1	Test Plan, Phase I Stringer-Reinforced Specimens	9
2	Phase II Spectrum Tests, Joint Tests and Two-Bay Panel Tests	12
3	Modified Compact Tension Specimen Fatigue Tests	36
4	Spectrum Tests of Single Lap Joint Specimens for Effect of Fastener Head Type	46

SECTION I

INTRODUCTION AND OBJECTIVES

For design of damage tolerant aircraft, it is necessary to perform fatigue crack-growth calculations of complex mechanically fastened structure containing designated preexisting cracks. The initial crack conditions designated in Reference 1 for cracks at fastener holes are a 1.3 mm (0.050 in.) fatigue-induced quarter-circular corner crack at the edge of the most critical hole, in all members joined by the common fastener, and 0.13 mm (0.005 in.) fatigue-induced quarter-circular corner cracks (continuing damage flaws) at all other hole locations.

A comprehensive experimental and analytical program was conducted to study the effects of varying the multiplicity and location of these small initial flaws in mechanically-fastened metallic structure. The crack path, growth rates, arrest times, and failure sequence were observed as they varied with initial crack condition. 7075-T6 Aluminum sheet, plate and extrusion were used on all tests. A total of 68 precracked structural specimens were fatigue tested to failure.

Crack growth predictions were made prior to testing these structural specimens using specific baseline da/dN data and stress intensity factors estimated from existing solutions by the method of compounding. Likewise the reinitialization time of a crack arrested at a fastener hole was predicted from fatigue baseline data and stress severity factors (λ) estimated by the compounding of known stress concentration factor (k_t) solutions.

This volume presents a summary of the overall test program and analysis performed as well as significant results obtained from the program.

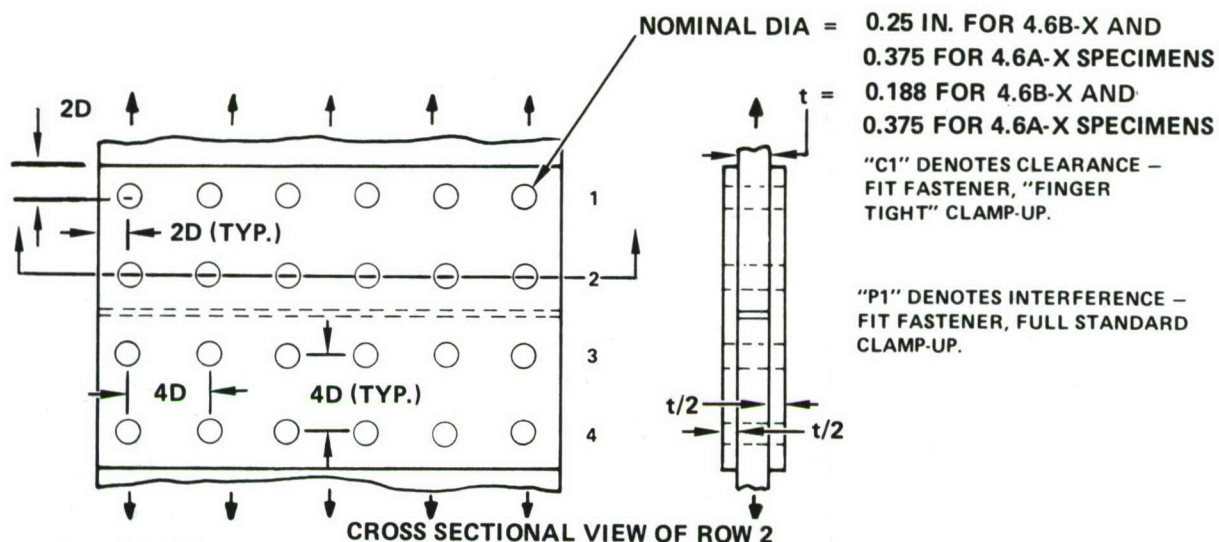
SECTION II

SUMMARY OF TESTS

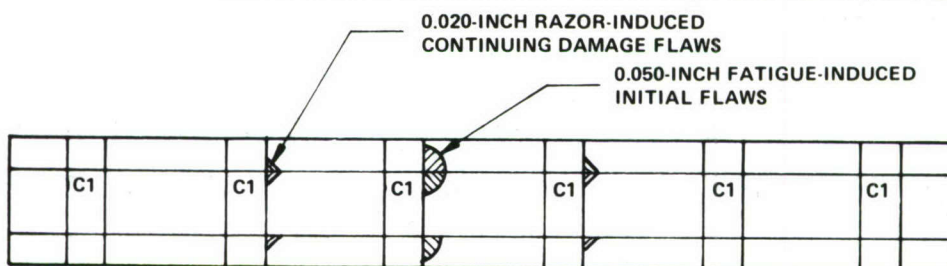
The test program consisted of two phases. Each phase included baseline testing, tests of precracked joints, and tests of precracked stringer-reinforced structure. Joints representative of chordwise splices and stiffened skins representative of wing structure were sufficiently diverse to meet the overall program objectives. The baseline testing in each phase was performed to support the analysis and testing methodology for the structural tests. Phase I tests consisted of constant amplitude fatigue tests designed to investigate the effect of the primary variables of interest: initial flaw locations, initial flaw multiplicity, continuing damage assumptions, and structural arrangement. Phase II tests were used to answer questions raised by the Phase I tests and to check that conclusions derived from the Phase I tests were valid for spectrum loading and for configurations of increasing complexity. All tests were used to assess the crack growth prediction methodology that would be used to comply with Reference 1. A crack growth analysis was performed for each Phase I test prior to the test results being available to the analyst.

1. PHASE I TESTS

Eighteen precracked chordwise splice specimens made from 7075-T6 Aluminum were tested in Phase I. The specimen configurations, shown in Figures 1 and 2, include two double-lap shear joints of different thicknesses and a single-lap shear joint. Steel Hi-lok fasteners with a large enough diameter to be bearing critical were used. Protruding-head fasteners were selected for the double-lap shear joints to simulate internal structure, whereas flush-head fasteners were selected for the single-lap shear joints to simulate external structure. The fastener spacing was 4 diameters, typifying standard design practice.



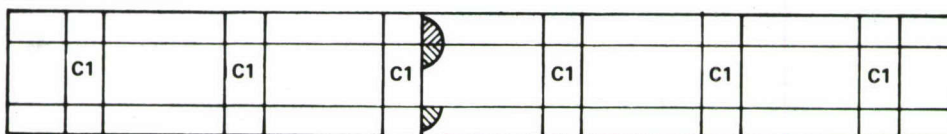
A. CONTINUING DAMAGE FLAWS, CLEARANCE – FIT HOLES, LOW CLAMP-UP, TRIPLE CRACK:



SPECIMEN
NUMBERS:

ROW	4.6A-1
2	4.6A-2
	4.6B-1

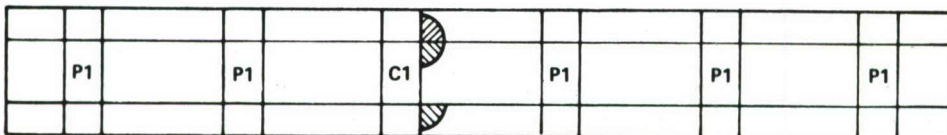
B. CLEARANCE – FIT HOLES, LOW CLAMP-UP, TRIPLE CRACK:



ROW

2	4.6A-3
	4.6A-4
	4.6B-2

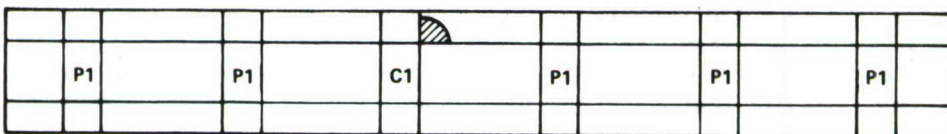
C. INTERFERENCE – FIT HOLES, STANDARD CLAMP-UP, TRIPLE CRACK:



ROW

2	4.6A-5
	4.6A-6
	4.6B-3

D. INTERFERENCE – FIT HOLES, STANDARD CLAMP-UP, SINGLE CRACK:



ROW

2	4.6A-7
	4.6A-8
	4.6B-4

Figure 1. Summary of Initial Damage Conditions, Double-Lap Shear Specimens

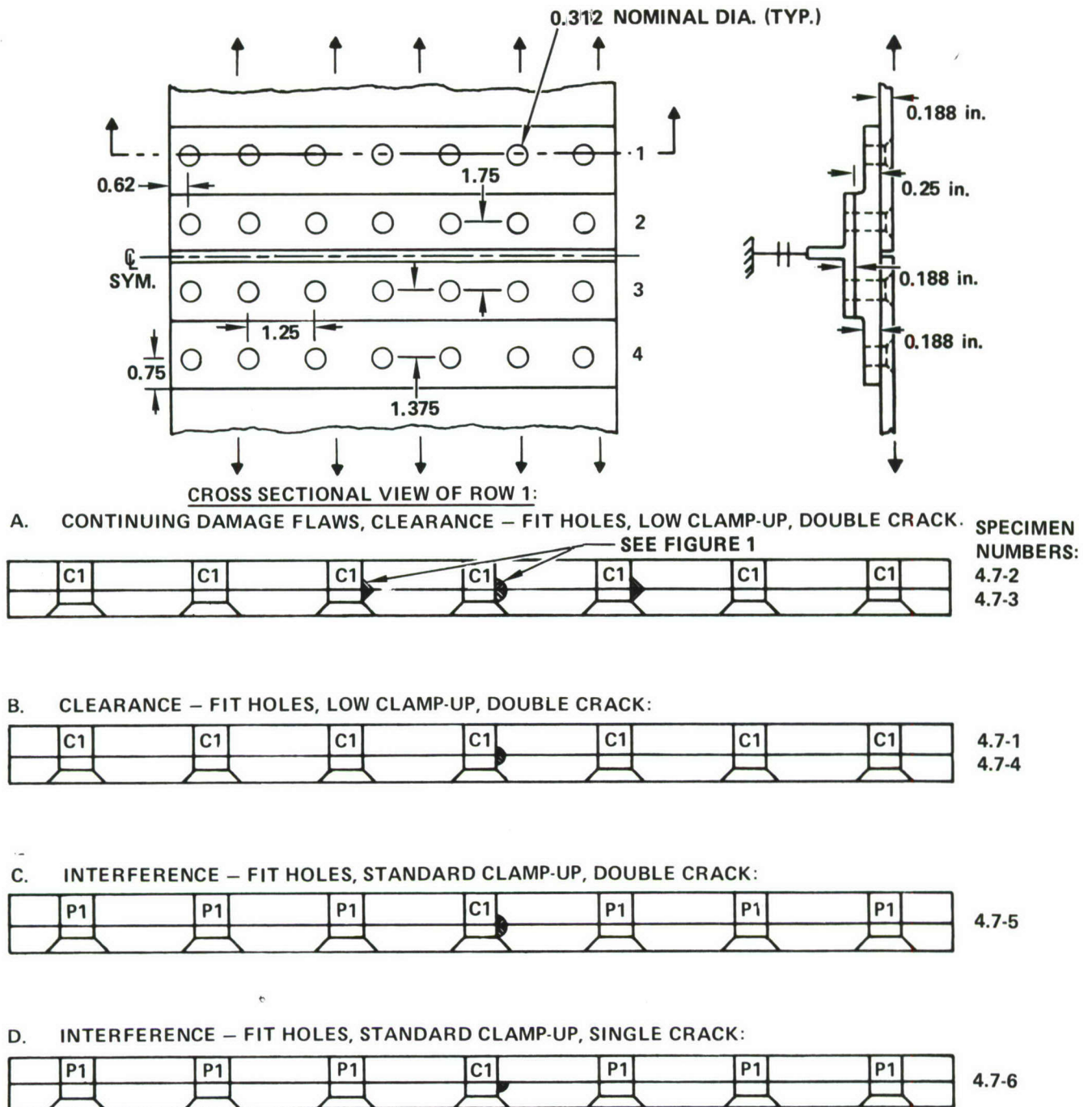


Figure 2. Summary of Initial Damage Conditions, Single-Lap Shear Specimens

This series of tests was conducted to demonstrate the difference in crack growth life for four different initial damage conditions. These four conditions, shown in Figures 1 and 2 are:

- A. Multiple 0.050-inch quarter-circular corner cracks (one in each member) at one fastener hole, simulated 0.005-inch continuing damage flaws at other critical fastener holes, and all fasteners clearance fit (C1) with no beneficial clamp up (finger-tight). This simulates the requirements of Reference 1.
- B. Same as A except no continuing damage flaws.
- C. Same as B except for fastening method used in unflawed holes. Standard fastener interference (P1) and standard clamp-up are used in all unflawed holes. The fastener at the precracked hole is C1 fit and finger-tight.
- D. Same as C except initial flaw is in one member only.

Note in Figures 1 and 2 that all initial flaws were induced at the faying surfaces rather than at the external surfaces, since peak stresses associated with fastener load transfer tend to be highest at the faying surface.

The 0.050 inch initial flaws were made as follows:

- Drilled a small hole at the right of the 0.050-inch crack location
- Made a starter notch with a razor blade
- Cycled the specimen to produce a fatigue crack of the desired length
- Drilled the hole of the proper diameter to leave a 0.050-inch quarter-circular flaw. The shape of the flaw made in this manner was fairly close to quarter-circular.

The continuing damage flaws were made 0.020 inch long with a sharp razor blade rather than fatigue induced 0.005 inch cracks. This was done because it was not feasible to fatigue-induce a controlled precrack at more than one fastener hole per structural member. Test results for various specimens and loading conditions shown in Figure 3 demonstrate that the crack growth period from a 0.020 inch razor flaw to failure is equivalent to the growth period from a 0.005 inch fatigue crack to failure.

The tests in Phase I included three configurations of stringer-reinforced test specimens. All the stringer-reinforced specimens tested were derived

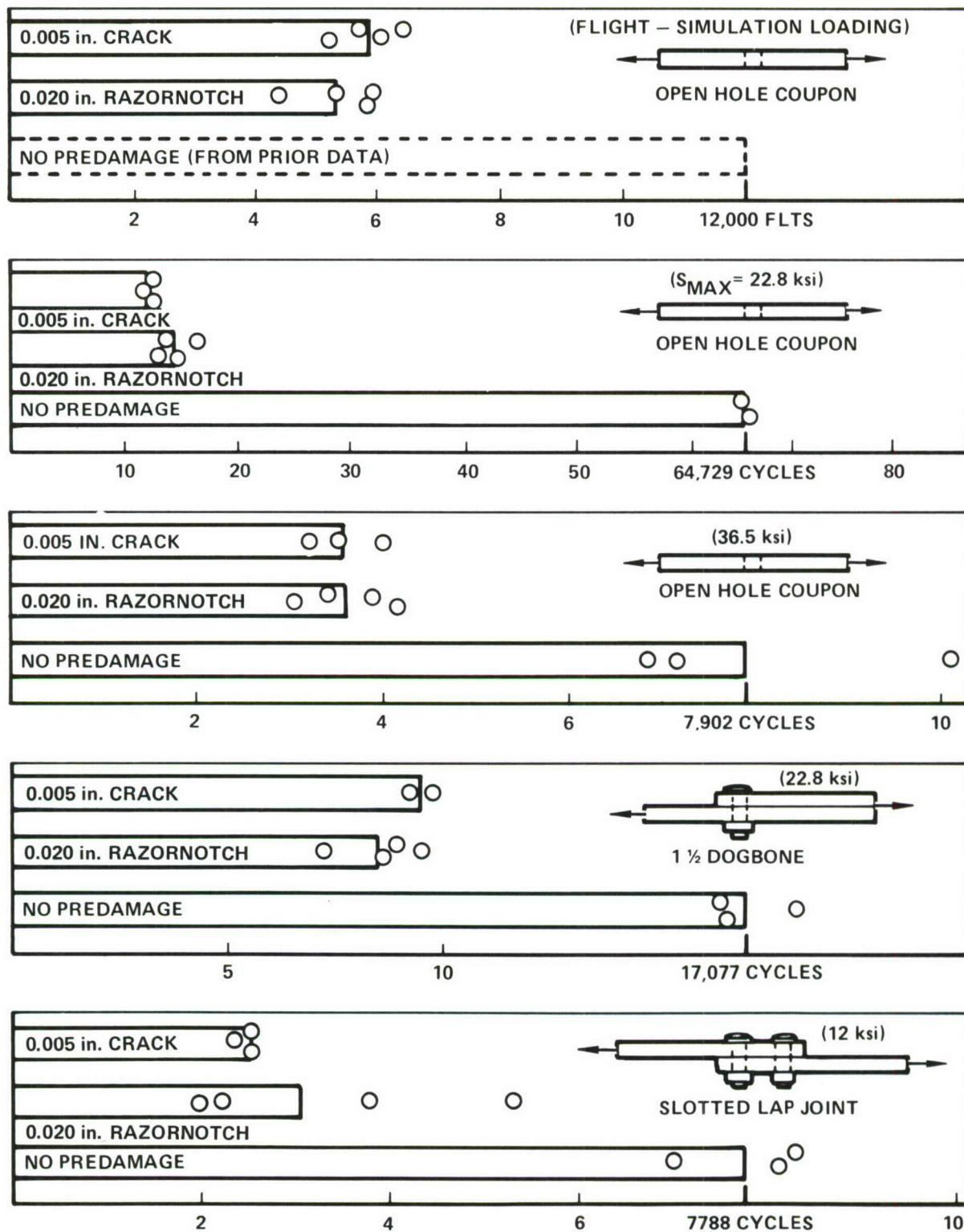
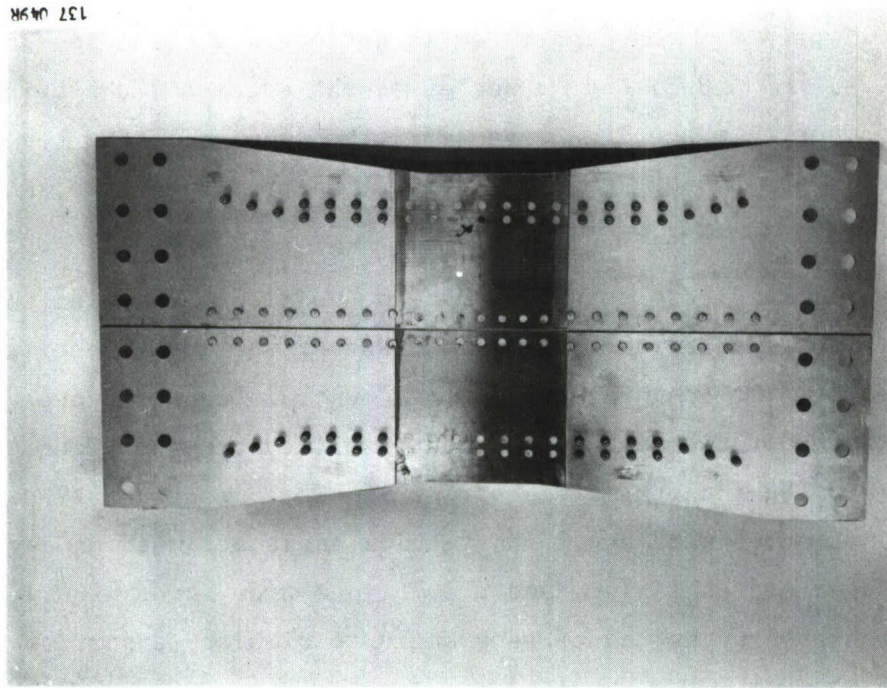
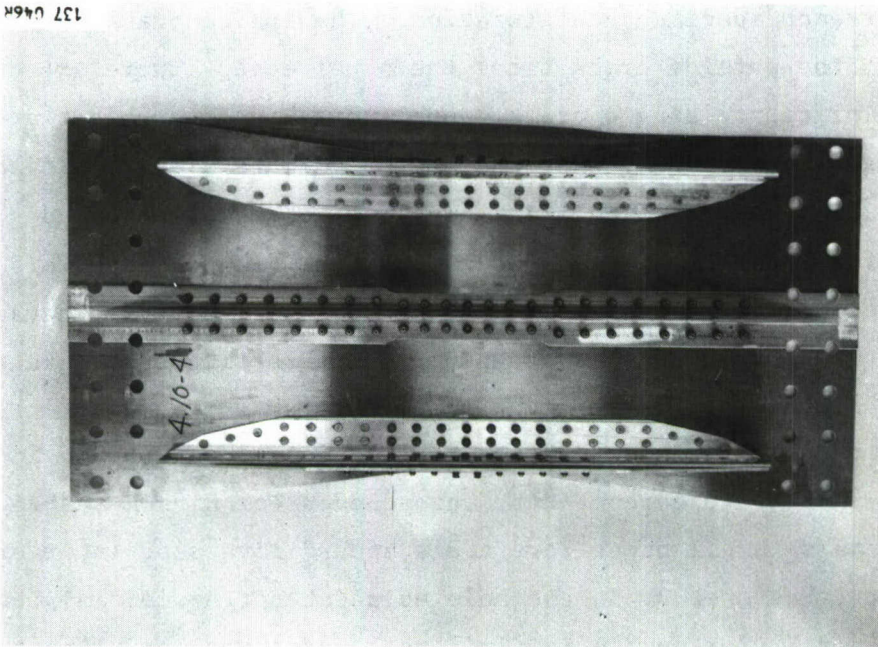


Figure 3. Summary of Test Results for Continuing Damage Flaws

from the basic 18 inch-wide two-bay configuration which was tested in Phase II. Photographs of the two-bay specimen are shown in Figure 4. For the edge-stiffened specimen (Type 4.9), the center tee is not present. The tee-stiffened specimens (Types 4.8-1 and 4.8-3) had no angles at the edges and the grip areas tapered out to 24 inches. In specimen type 4.8-1 the skin under the tee was continuous, whereas in the two-bay panels and specimen type 4.8-3 the skin under the tee was split.

All stringer-reinforced test specimens had an overall nominal length of 44.5 or 47.5 inches and were 18 inches wide in the test section. Specimen type 4.8-1 consisted of a 0.188 inch sheet with a central tee stringer. Specimen type 4.8-3 consisted of two 0.188-inch sheets spliced together longitudinally across the base of a 0.188 inch-thick tee stringer. Specimen type 4.9 consisted of a 0.188 inch sheet with a 0.25 inch-thick angle stringer on each edge to simulate a spar cap on a wing, and a 3.25 inch-wide strip of 0.188 inch sheet attached to the protruding leg of each angle to simulate a portion of the shear web.

Twelve each of specimen types 4.8-1, 4.8-3, and 4.9 were tested in Phase I for a total of 36 Phase I stringer-reinforced specimens. The Phase I test plan for these specimens is summarized in Table 1. There are two basic flaw locations identified for each specimen configuration. The inside crack faces the center of the panel; the outside crack faces the panel edge. There are three levels of flaw multiplicity: single crack, double crack, and double crack with continuing damage flaws. Note that there are two more single initial crack cases for the edge-stringer specimens than for the tee-reinforced specimens, and two fewer replications of double initial flaw cases. This reflects a change made during the program because the single initial damage cases were found to have provided some of the more interesting test data for the center-stringer specimens. In addition, test scatter was low for this type of specimen, limiting the need for replication. Fastener 1, in the precracked hole, is always a clearance-fit, untorqued steel Hi-lok fastener, and the remote fasteners in all other rows are standard rivets or interference-fit Hi-loks. However, Fastener 2, in the hole adjacent to the initial crack, is either like Fastener 1 (for double initial crack cases with or without continuing damage flaws) or like the remote fasteners (for single or double initial crack cases without continuing damage flaws).



(a) Front View

(b) Back View

Figure 4. Two-Bay Stringer-Reinforced Specimen

TABLE 1. TEST PLAN, PHASE I STRINGER-REINFORCED SPECIMENS

Specimen Type	INITIAL FLAWS	SPECIMEN NUMBERS					
		Fastener 2			Fastener 2		
		Same as Fastener 1			Same as Remote Fasteners		
		Double Initial Flaws, F_1, F_2			No Continuing Damage Flaws		
		Continuing Damage Flaws 0.005 Inch	No Continuing Damage Flaws	Double Initial Flaws F_1, F_2	Single Initial Flaw F_1 Only	Single Initial Flaw F_2 Only	
Center Stringer Continuous Skin Type 4.8-1 - X	INSIDE	4.8-1-1 4.8-1-2	4.8-1-3 4.8-1-4	4.8-1-5	4.8-1-6		
	OUTSIDE	4.8-1-7 4.8-1-8	4.8-1-9 4.8-1-10	4.8-1-11	4.8-1-12		
Center Stringer Split Skin Type 4.8-3 - X	INSIDE	4.8-3-13 4.8-3-14	4.8-3-3 4.8-3-4	4.8-3-5	4.8-3-6		
	OUTSIDE	4.8-3-9 4.8-3-10	4.8-3-7 4.8-3-8	4.8-3-11	4.8-3-12		
Edge Stringer Type 4.9 - X	OUTSIDE	4.9-1 4.9-2	4.9-3	4.9-5	4.9-6	4.9-4	
	INSIDE	4.9-7 4.9-8	4.9-9	4.9-11	4.9-12	4.9-10	

Fastener 1 was flush head steel Hi-lok, clearance fit, low fastener torque.

F_1 and F_2 were nominally 0.050 inch quarter circular-shaped fatigue cracks.

Razor flaws of 0.020 inch were used to simulate fatigue-induced 0.005 inch continuing damage flaws.

All specimens constant-amplitude cycled at $S_{MAX} = 17$ ksi, $R = 0.1$.

Clearance-fit steel Hi-lok fasteners were used in the flawed holes. Fasteners in the six rows nearest the center of the specimens were selected to be representative of standard design practice for each configuration. Thus interference-fit steel flush-head fasteners were used where the specimen simulates a skin-to-skin splice (Specimen type 4.8-3) or skin-to-web splice (Specimen type 4.9), whereas flush-head aluminum rivets were used where there was no splice (4.8-1 type specimen). Protruding head fasteners were used at the remaining locations between grips because these fasteners have good fatigue characteristics, are easy to install and are sufficiently removed from the test section so as not to influence the crack growth results.

Doublers were bonded to each end of the specimens to provide a gradual transition from the test section to the end grips without introducing appreciable bending stresses. The specimens were also necked down so that the combined bending and axial stresses in the transition sections were less than in the test section. To further minimize the possibility of fatigue failures in the grip area, clamp-type end attachments were used. The tee stringer was tapered down in the grip area, so that only its base projected into the grip area. This resulted in induced bending stresses. The edge stringers, being of greater cross section, were directly picked up by the grips through pairs of aluminum channels clamped to the protruding legs of the angles and the simulated shear webs.

The 0.050 inch fatigue-induced flaws in the plate (skin) members were made using the same procedure as for the joint specimens. For the extrusion members fatigue cracks were induced using either tension loading (tee members) or pin loading at the flaw location (angle members). It was not feasible to apply bending stresses of the proper magnitude at the flaw location without inducing compressive yielding at the top of the vertical leg of the angle or tee member. The size of the initial flaw for both angles and tees was larger on the hole surface than along the skin surface. Also, the crack surface was oriented at a slight angle to the plane perpendicular to the longitudinal axis of the specimen.

The Phase I specimens were fatigue tested in a 200-kip MTS machine with a controlled laboratory air environment (69° - 75°F, 30 - 50% RH). Axial loads were applied to pin end attachments bolted to the specimens. The specimens were cyclically loaded until complete failure occurred. A maximum stress

of 17 ksi and a stress ratio of 0.1 was used in all cases. Intermittently, blocks of marking cycles were applied to the first few joint specimens at $S_{\max} = 17$ ksi and $R = 0.82$. However, the marking cycles did not mark the fracture surface successfully, and the process was abandoned for the remainder of the joint tests.

Each of the two-bay and edge-stringer specimens was loaded by means of steel plates that clamped to the skin, and pairs of aluminum channels that clamped through the simulated shear web and outstanding leg of the angle. By directly picking up the stringers in this manner, the out-of-plane bending was somewhat alleviated. Two large beams spanning the columns of the MTS machine were connected through flexures to a double rectangular frame which clamped directly onto the specimen. According to the strain gage readings, little transverse bending occurred in the Phase II two-bay specimens. Some bending occurred in the edge stringer specimens; however, the distribution of stress through the thickness was typical of the stress distribution in aircraft wing structure.


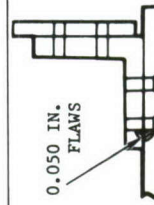
2. PHASE II TESTS

The Phase II test program included fourteen flight simulation spectrum tests as shown in Table 2. The purpose of the spectrum testing was to establish the extent to which structural effects and load history effects can be considered independently in crack growth analysis of complex structure. In addition to the baseline tests, there were duplicate tests for each of the structural configurations.

The test spectrum was 80-flight random cycle sequence that simulated the lower wing surface loads in the spanwise direction, excluding compression, for a typical fighter aircraft during a pilot training course. The largest load factor, 7.2, which occurs in flight number 39, is the reference load factor for the sequence. Most of the tests were conducted at a reference stress of 30 ksi, which is a typical design stress at limit load for 7000 series aluminum alloys. The application of the reference load tended to visibly mark the fracture surface, thus providing a history of the crack front shape and (by the spacing of the marks) crack growth rate for cracks hidden within the structure.

To clarify the role of fastener head type on the reinitiation time of a crack arrested at a fully-torqued, interference-fit Hi-lok fastener, two of

TABLE 2. PHASE II SPECTRUM TESTS, JOINT TESTS AND TWO-BAY PANEL TESTS

Specimen Configuration	Specimen No.	Type of Loading	Reference Load or Stress	Damage Condition	Comments	
CT Specimen (Baseline da/dN)	CT5-1	Spectrum	1.6 kip	No preflaw	ASTM compact tension specimen with $W = 5$ in.	
	CT5-2		1.0 kip			
Modified CT (Baseline Crack Initiation)	MCT-1	Spectrum	1.8 kip	No preflaw	ASTM compact tension specimen modified with a 0.125 in. radius hole at end of slot, $k_t = 65.4$	
	MCT-2		1.8 kip			
	MCT-3		3.125 kip			
	MCT-4		3.125 kip			
Split Skin Tee	4.8-3-1	Spectrum	30.0 ksi	Same as Specimen Nos. 4.8-3-3 and 4.8-3-4, Table 1	Hi-Lok HL51-10 flush-head fasteners	
	4.8-3-2		30.0 ksi			
Double Lap Joint (Figure 1)	4.6A-9	Spectrum	30.0 ksi	Same as Specimen Nos. 4.6A-3 and 4.6A-4, Figure 1B	Hi-Lok HL50-12 protruding-head fasteners	
	4.6A-10		30.0 ksi			
Single Lap Joint (Figure 2)	4.7-10	Spectrum	25 ksi	Figure 2D	Hi-Lok HL51-10 flush-head fasteners	
	4.7-11		30 ksi			
	4.7-12	Spectrum	30 ksi	Figure 2D	Hi-Lok HL50-10 protruding-head fasteners	
	4.7-13		30 ksi			
Two-Bay (Figure 4)	4.7-7	Constant Amplitude	$S_{max} = 17$ ksi,		Fasteners: Pl fit, full torque except the following, which were C-1 fit, low torque: <ul style="list-style-type: none">The six skin-stringer fasteners in the initial crack planeThe eight web-stringer fasteners adjacent to the initial crack plane.	
	4.7-8		$R = 0.1$			
	4.10-1	Constant Amplitude	$S_{max} = 12$ ksi,			
	4.10-2		$R = 0.1$			
4.10-3	Constant Amplitude	$S_{max} = 12$ ksi,				
4.10-4		$R = 0.1$				

the single lap joint specimens (4.7-7 and 4.7-8, Table 2) were fabricated and constant amplitude tested identically to Specimen 4.7-6 (Figure 2), except that protruding head rather than flush head Hi-lok fasteners were used. For similar reasons, two of the single lap joint specimens shown in Table 2 with flush head and two with protruding head fasteners were spectrum tested using the 80-flight spectrum discussed above. The two-bay tests included specimen geometries and precrack geometries identical to two of the split-skin tee specimens tested except for the addition of edge stiffeners and simulated shear web strips, and geometries identical to two of the edge-stringer specimens except for the addition of a central tee stiffener and the split in the skin. As such, they are excellent tests for evaluating the effects of increased structural complexity. In addition, a lower stress level (12 ksi as opposed to 17 ksi) was used on half of the two-bay tests to investigate the effect of stress level on the crack growth behavior and to insure that multistringers interaction effects would be present.

The Phase II tests were conducted as discussed above under Phase I tests.

SECTION III

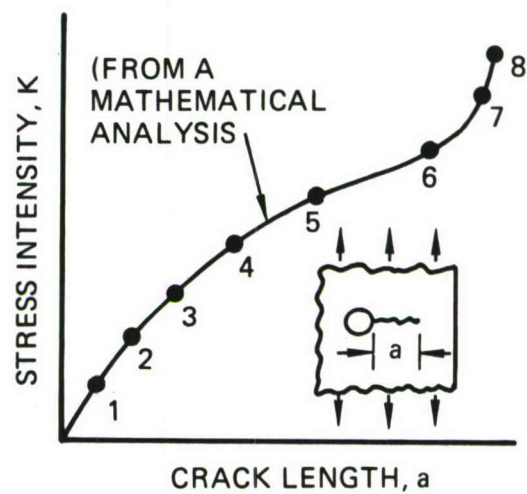
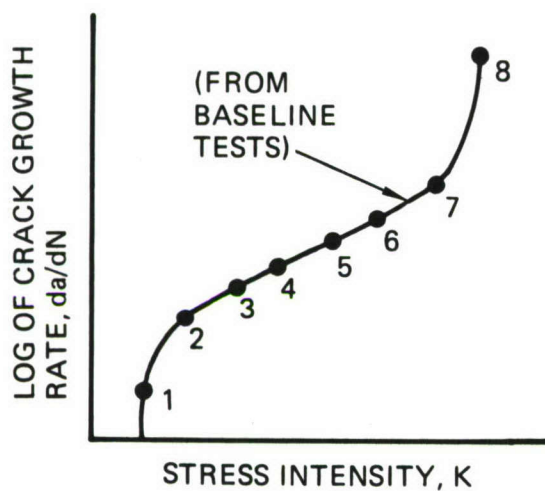
SUMMARY OF ANALYSIS

Fatigue crack growth analyses were performed for all the initially flawed specimens prior to testing. The method of analysis consisted of the steps shown in Figure 5. Baseline crack growth rate data (da/dN vs K) was obtained from test data for the appropriate material, loading, and environment as shown in Figure 6. The crack length and the stress intensity factor (K vs a) curve for the geometry of the cracked structural member was obtained from available or derived solutions. By combining these two and integrating dN/da , predictions were made of the number of cycles required to reach a defined crack length "a." A limitation on this analysis procedure is that inelastic deformations must be limited to the immediate crack tip neighborhood (small-scale yielding).

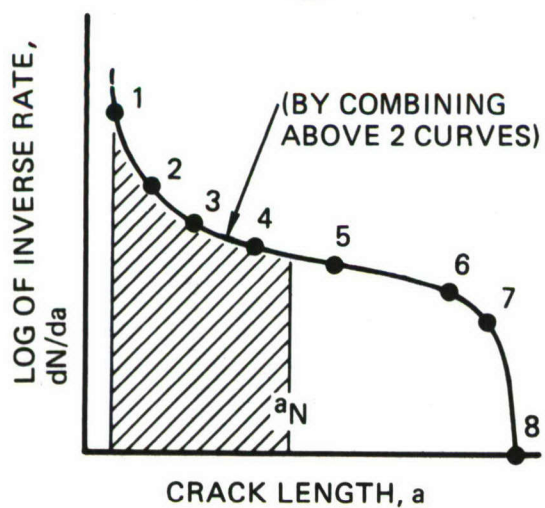
In mechanically fastened structure the problem of crack growth prediction requires additional considerations. As the crack grows, the fastener loads will, in general, change. This change could be important since the fastener load distribution affects the magnitude of the stress intensity factor. Furthermore, the propagating crack may be arrested at a fastener hole or free edge. If no flaw is present at the opposite side of the arresting hole, then crack reinitiation time must be predicted.

The phenomenon of crack arrest and reinitiation was studied in Reference 2. It was found that the reinitiation time of a crack, arrested at an unflawed empty hole can be estimated using fatigue data from center-notched (unflawed) coupons. This begins by estimating the stress concentration factor k_t for the long notch created by the arrested crack. Then by matching both the peak elastic stress ($k_t S$) and the notch radius with those of the baseline fatigue coupon, the crack initiation times also match. The results of the baseline fatigue tests, plotted in Figure 7, show that the data fits a linear relationship

1



2



3

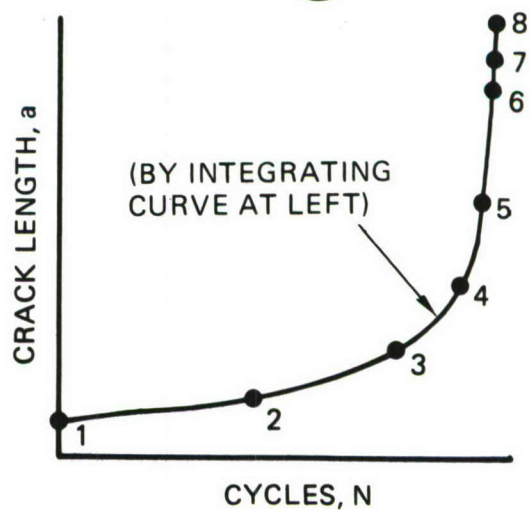


Figure 5. Crack Growth Prediction Method

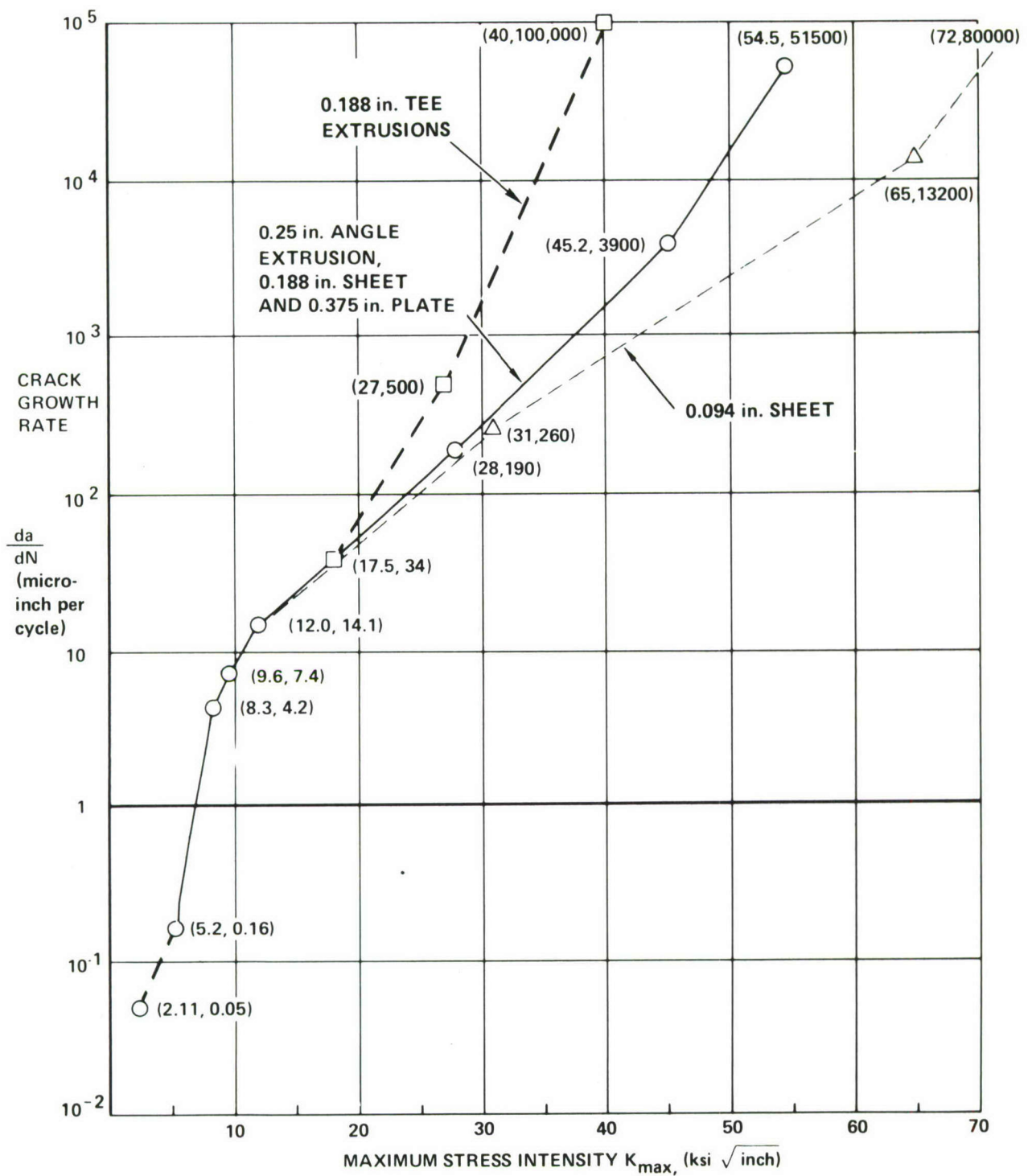


Figure 6. Summary of Fatigue Crack Growth Data, 7075-T6 Aluminum, $R = 0.1$, Laboratory Air Environment

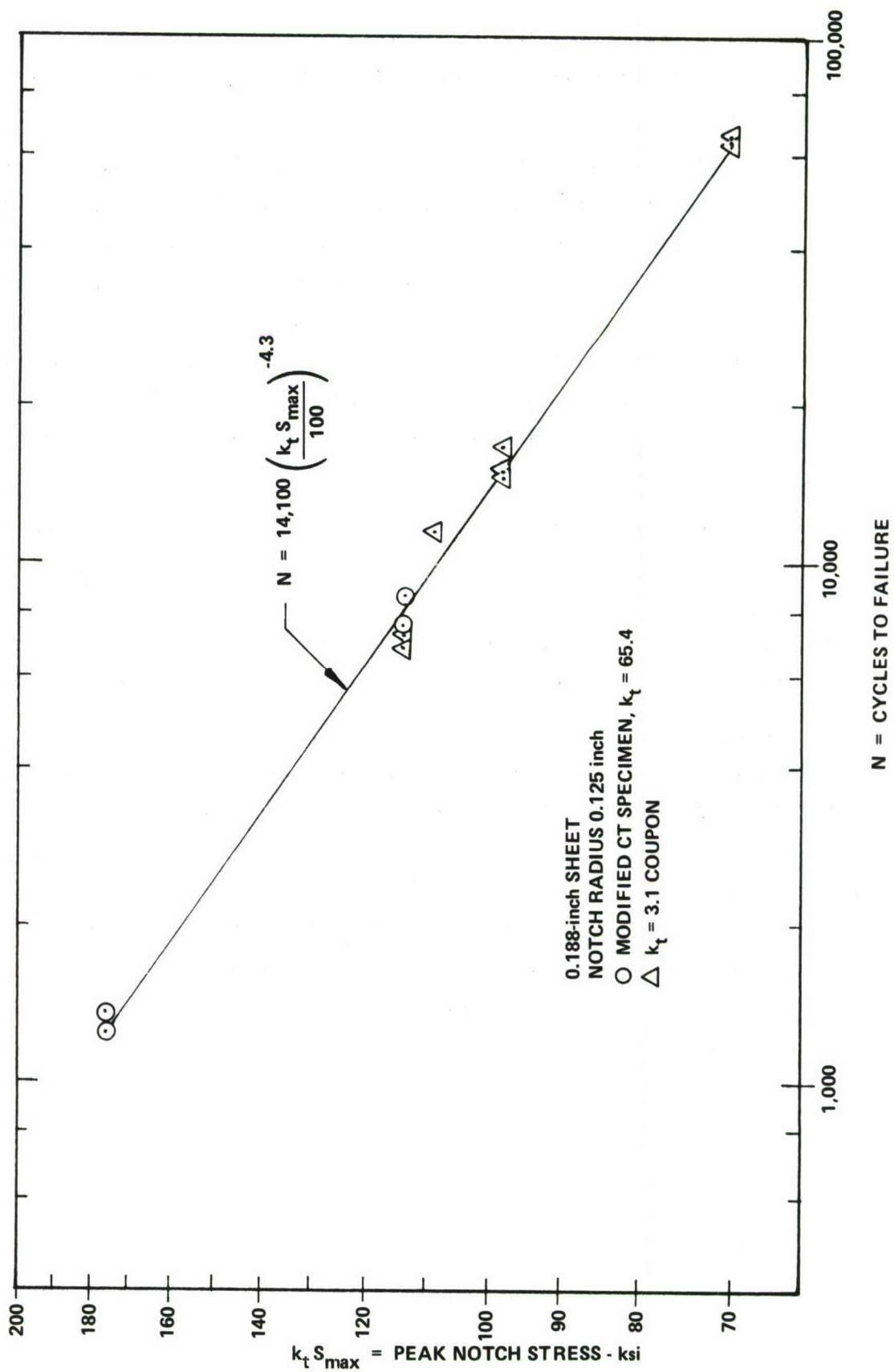


Figure 7. S-N Curve for 3/16 Inch 7075-T6 Aluminum Sheet, $R = 0.1$

between $k_t S_{\max}$ and N in log-log space. This relationship was used for predicting the crack reinitiation times at unflawed notches in the various test specimens.

The stress severity factor (SSF) concept (Reference 3) was used to account for the effect of fastener load transfer in predicting crack reinitiation at fastener hole locations. The stress severity factor is equivalent to a k_t value which accounts for hole quality and hole size (α), fastener types and fastener fit (β), and fastener rotation and deflection (θ). The values of α and β were determined empirically using baseline fastener fatigue specimens. The values of θ were derived from the results of finite element analyses. For prediction of crack reinitiation times, the value of SSF replaces the value of k_t in the equation given on Figure 7.

Crack reinitiation times had to be predicted for cases where one end of the crack was growing while the other end of the crack was arrested at a fastener hole. In this case there is a continuous change in the stress severity factor for the initiating crack. Therefore the damage rate at the hole changes, and it was necessary to do a linear cumulative damage analysis.

The baseline fatigue data provided a relationship between damage rate dD/dt (equal to inverse fatigue life, $1/N$) and the stress severity factor. Equations were derived to obtain the stress severity factors as a function of crack length. The results of the crack growth computation for the growing crack provided crack length as a function of time. Combining these three, the damage rate was expressed as a function of time. Integration then resulted in the required estimate of the number of load cycles N_i required to accumulate sufficient damage D_i on the uncracked side of the hole to form a fracture mechanics crack; viz.,

$$\int_0^{N_i} \frac{dD}{dt} dt = D_i \quad (1)$$

A crack of about 0.050 inch was assumed to be a fracture mechanics crack (i.e., one whose growth was estimated using linear elastic fracture mechanics methods). The baseline data that formed a basis for estimating damage rate was from coupons which cracked beyond 0.050-inch and failed completely when the damage was 1.0. Back-calculating crack growth in some of these coupons showed that typically a 0.050-inch crack is formed at about 85 percent of the observed specimen failure life. Therefore a 0.050-inch crack is assumed to be initiated when $D_1 = 0.85$. Thereafter a da/dN analysis was applied to the initiated crack, using baseline da/dN data and the appropriate stress intensity equations.

Finite element analyses were used to determine the fastener loads in the structural joint specimens. The fastener load at the flaw origin is of particular interest because it most strongly affects the early growth of the crack. Regardless of crack length, this load is zero in the stringer-reinforced panels because the crack plane is a plane of symmetry. However, it is nonzero in the structural joint specimens, and can vary with crack size.

The distribution of fastener loads in a damaged joint is influenced by the extent of damage and by transverse bending deformations of both the fasteners and the joint. Since the cracking and the bending occur in different planes, the structural analysis of such joints is a three-dimensional problem.

By the approach employed here, approximate solutions for the fastener load distribution were obtained for various assumed damage conditions. Two different types of two-dimensional finite element analysis were conducted.

In the first type of analysis the two-dimensional model corresponds to a view of the joint, where the stretching and transverse bending of the joint and all the deformations of the fasteners can be viewed. From this profile view the widthwise details of the specimen, including the crack length itself, cannot be modeled. However, the two-dimensional finite element model corresponding to this profile view can be used to obtain effective fastener stiffnesses for the second analysis model. Those effective stiffness values are intended to account for the transverse deformations of the fastener and the joint itself.

In the second type of analysis, the two-dimensional model corresponds to a top view of the joint. From this view the (through-the-thickness) crack was visible and all of the fasteners were modeled separately. Each fastener was assigned an effective stiffness value as obtained from the first analysis. The crack length was selected and the fastener loads were calculated using the NASTRAN System.

SECTION IV

SUMMARY OF RESULTS

1. PHASE I RESULTS

Figure 8 shows the effect of continuing damage flaws on total life of the Phase I specimens. The continuing damage site located in the same hole as the primary 0.050-inch crack, but diametrically opposite, was the most critical location for continuing damage. If continuing damage flaws are not placed there, they will usually initiate there as an early step in the failure sequence. The presence of continuing damage flaws had very little effect on the crack growth lives of the double-lap joints, single-lap joints, or tee-reinforced continuous-skin specimens with initial cracks located "inside" (see sketch in figure). However, none of these had a continuing damage flaw at the most critical location. Conversely, there were continuing damage flaws at this critical location in the tee-reinforced, continuous-skin specimens with outside cracks and in the spanwise splice specimens. The presence of these flaws led to significantly shorter crack growth lives.

The effect of continuing damage flaws for the edge stiffened specimens in Figure 8 does not appear to affect the crack growth life significantly. This is understandable for Specimens 4.9-7 and 4.9-8 since the skin crack was the critical location determining life. The continuing damage flaws in the angle member affect the later growth rate of the angle flaw which in turn affected the growth rate of the critical skin crack. However, the secondary effect on the growth of the skin crack occurred near the end of the life so it had little overall effect on total life.

The results of Specimen 4.9-2 seem to be contrary to the conclusion that continuing damage flaws opposite the critical initial flaw location will significantly shorten the crack growth life. For reasons that seem not to be

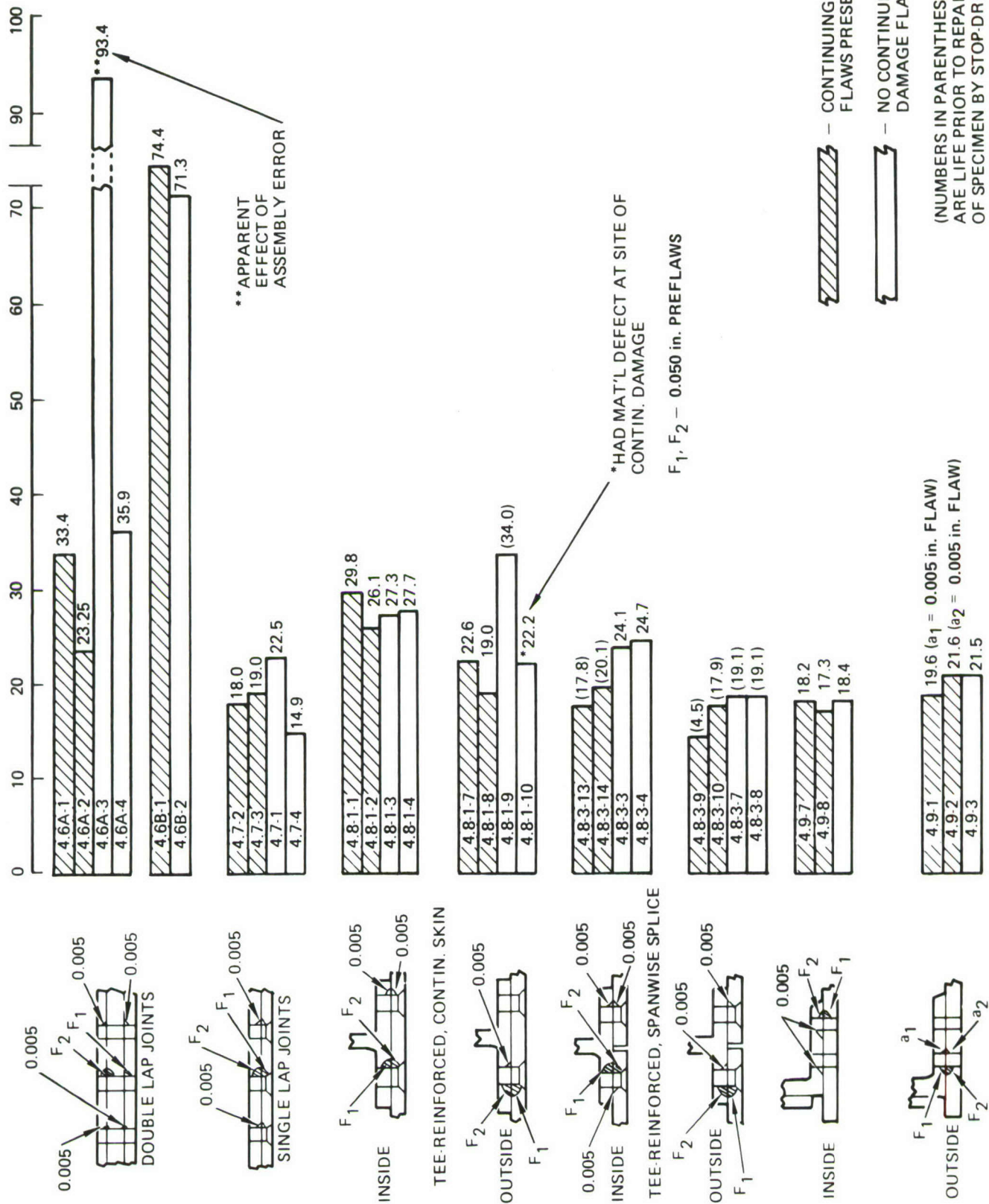


Figure 8. Effects of Continuing Damage Flaws on Life

relevant to the flaw locations, the main skin crack in Specimen 4.9-2 grew slowly and took about 3000 cycles longer to arrest at the edge as the first step toward failure. This counterbalanced any effect of the continuing damage flaws.

MIL-A-83444 requires that fasteners should be considered to be clearance-fit and untorqued; that is, no benefits of clamp-up and interference can be included in the crack growth analysis, either for the primary fastener (site of the 0.050-inch cracks) or for the secondary fasteners.

Figure 9 compares crack growth lives for specimens with lightly torqued, clearance-fit secondary fasteners and otherwise identical specimens with secondary fasteners installed by standard methods. In the joints, the crack growth lives were greatly enhanced when the standard interference fit and torque were applied to all secondary fasteners. Crack growth rates were slower, but more notably, the cracks were arrested for very long times at the two fully torqued, interference fit fasteners on either side of the crack-origin fastener. The long arrest times were attributed primarily to fastener torque, which created substantial frictional forces between the fastener head or collar and the cracked piece. These friction forces reduced the amplitude of the cyclic deformations in the neighborhood of the tip of the arrested crack.

Conversely, in the tee-reinforced specimens the effect of fastener type and/or installation method was insignificant. By the time the crack was arrested at the secondary fastener the protruding leg of the tee (and therefore nearly all of the tee) was ususally broken. With such extensive damage, the arrest time and remaining life was small regardless of the fastener-torque or type of fastener used in the second fastener hole.

The fastener type and/or installation also had little effect on the crack growth life for the edge-stiffened specimens. Specimen 4.9-11 was critical for the skin crack which reached the end of life before the crack initiated on the opposite side of crack F_1 and grew to the secondary fastener hole. Specimens 4.9-3 and 4.9-5 were critical for cracking of the angle member. By the

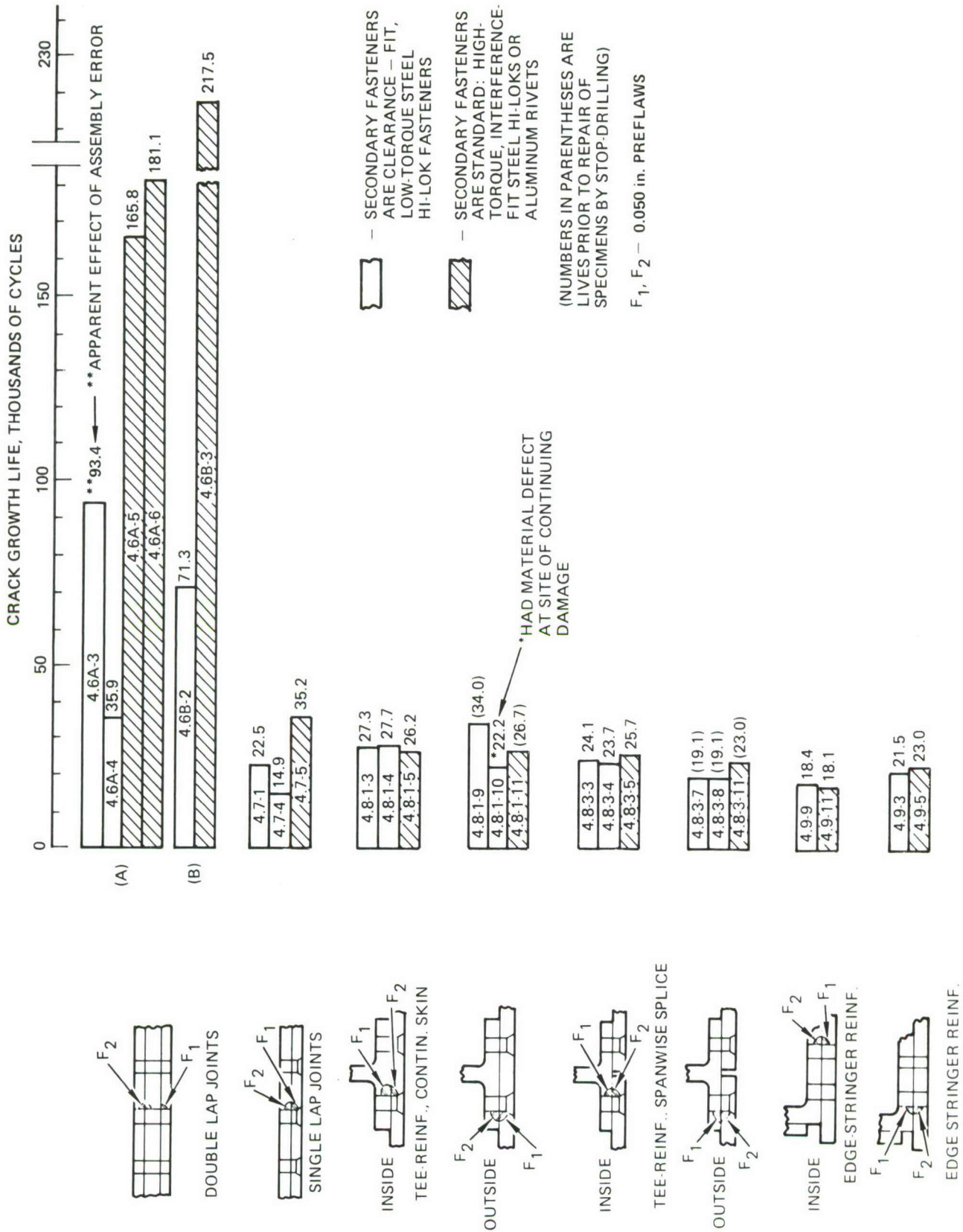


Figure 9. Effects of Fastener Type on Total Life

time the crack in the angle and the skin reached the secondary fastener location in both specimens, it was near the end of the life of the specimen (i.e., the angle was nearly broken). In this case the fastener-torque or type would have very little effect on the total life.

Figure 10 shows the difference in life between identical specimens with cracks in all members joined at a common fastener and a crack in just one member. In the single and double lap joints there was not significant difference in life due to the number of initial flaws. In the double lap joints the long arrest times dominated the test results and hid any effect of the number of initial flaws. In the single lap joint, the initial double crack did not propagate because doubler stresses in the first fastener row are low. Furthermore, the specimen fails as soon as one member (the skin) fails. Therefore there was no significant difference between the single lap joint specimen with initial skin and doubler cracks and the specimen with only a skin crack.

Conversely, Figure 10 shows a significant effect of single (instead of double) initial cracks in the tee-reinforced specimens. In these cases the nominal stresses were equal in both the tee and the skin members so both initial cracks propagated if present. Furthermore all members must fail when the specimen fails. Both are ample reasons to expect the effects shown in Figure 10.

The edge-stiffened specimens also had longer crack growth lives for single initial cracks except for Specimen 4.9-12. The effect of initial crack F_2 on the life of Specimen 4.9-11 was small because the skin crack grew to a critical size (stopped drilled size) before the crack initiated on the opposite side of initial crack F_2 in the angle.

Two different initial flaw locations (inside and outside cracks, Figure 11) were investigated in the tee-reinforced specimens. The inside crack was expected to cause the earliest possible failure of the tee. The outside crack was expected to minimize the beneficial effects of the tee reinforcement on crack growth in the skin. Hence, before the tests were conducted it was unclear which initial crack location would lead to shorter crack growth lives.

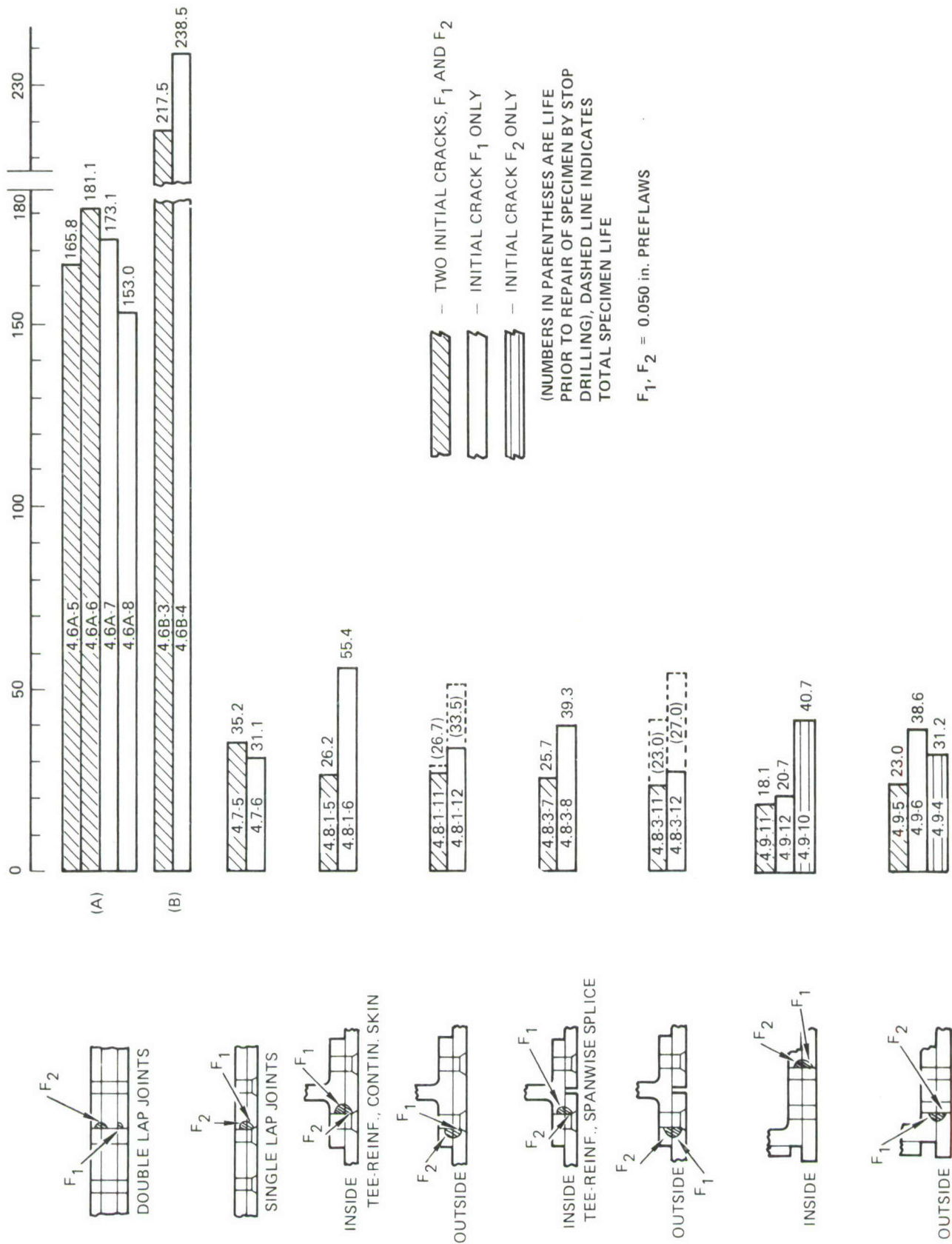


Figure 10. Effects of Single and Multiple Initial Cracks

Figure 11 compares the lives of specimens with corresponding inside and outside initial crack conditions for tee-stiffened specimens. The comparisons are made for both continuous skin and spanwise splice-type specimens and for each of the four levels of initial damage.

The outside cracks were more critical for continuous skin specimens with continuing damage flaws and double initial cracks. The cause seemed to be the location of continuing damage flaws; the outside crack case had a continuing damage flaw on the opposite side of the hole with the primary precrack, while the inside crack case did not. When the continuing damage flaws were omitted (double initial crack cases) the inside crack case was more critical. However, the single outside skin crack turned out to be substantially more critical than the inside tee crack.

Outside cracks were always more critical than inside cracks in the spanwise splice-type specimens. For both inside and outside cracks a continuing damage flaw was located on the opposite side of the precracked hole, so that an equal degree of severity was introduced by the addition of continuing damage flaws. The single initial outside crack in the skin progressed to failure faster than the single initial inside crack in the tee.

The effect of inside and outside preflaws on the crack growth life of edge-stiffened members is shown in Figure 12. For double initial cracks, the inside location is more critical than the outside location. Inside crack location F_1 is the most critical location for an initial crack. This is comparable to the result obtained for a spanwise splice tee-reinforced specimen where the single initial crack location F_1 had about the same life as the double crack configuration. Both were cracks in the skin growing away from the region of influence of the stiffener. Single initial cracks in the angle member (angle-stiffened specimens) or tee member (tee-stiffened specimens) were not as critical as double initial cracks or single initial cracks in the skin growing away from the stiffener.

The tests were run at just one stress level. The comparisons presented in Figures 8 through 12 will not necessarily apply generally to all stress levels or to other structural configurations.

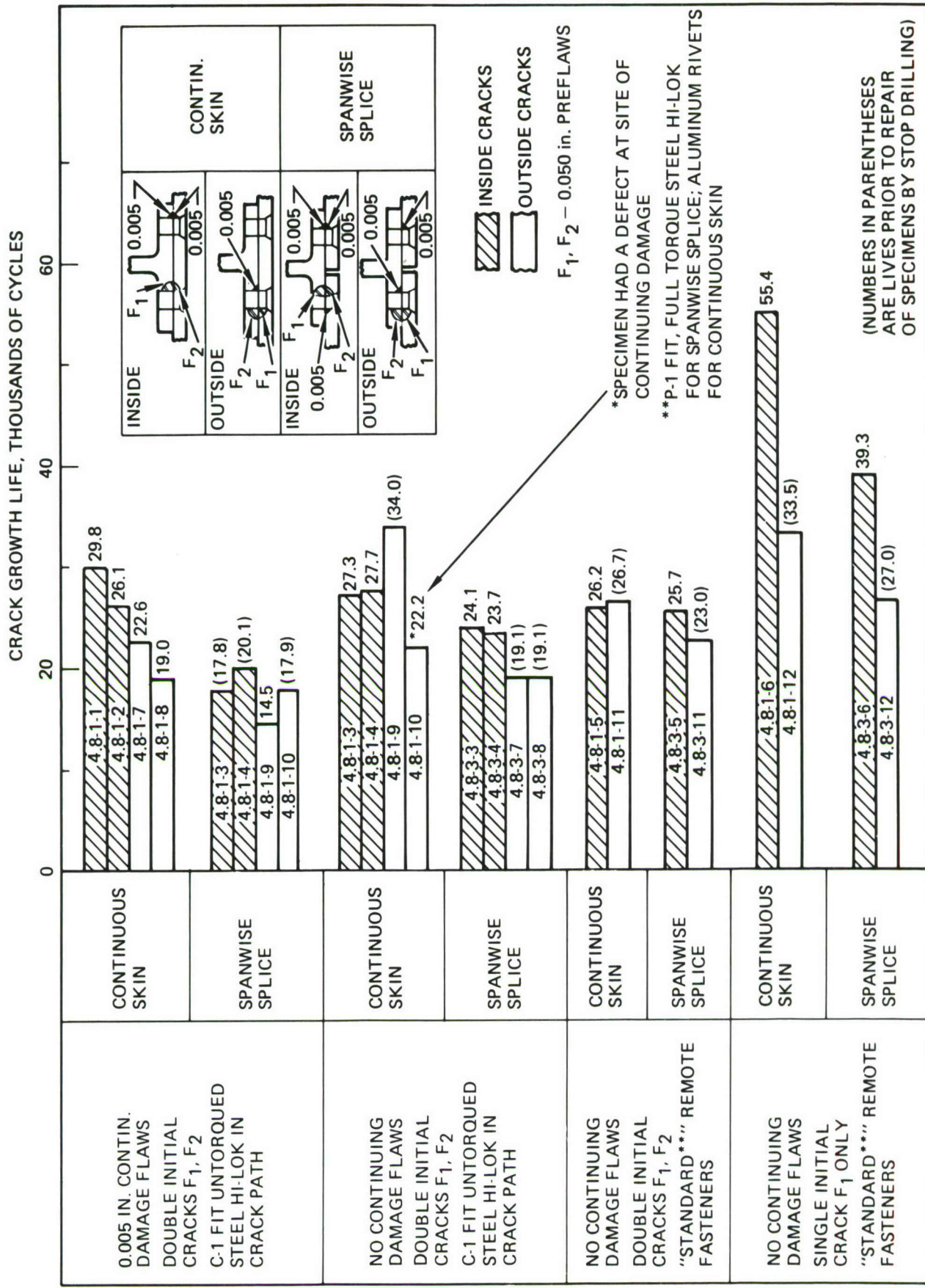


Figure 11. Comparison of Alternate Flaw Locations, Tee-Reinforced Specimens

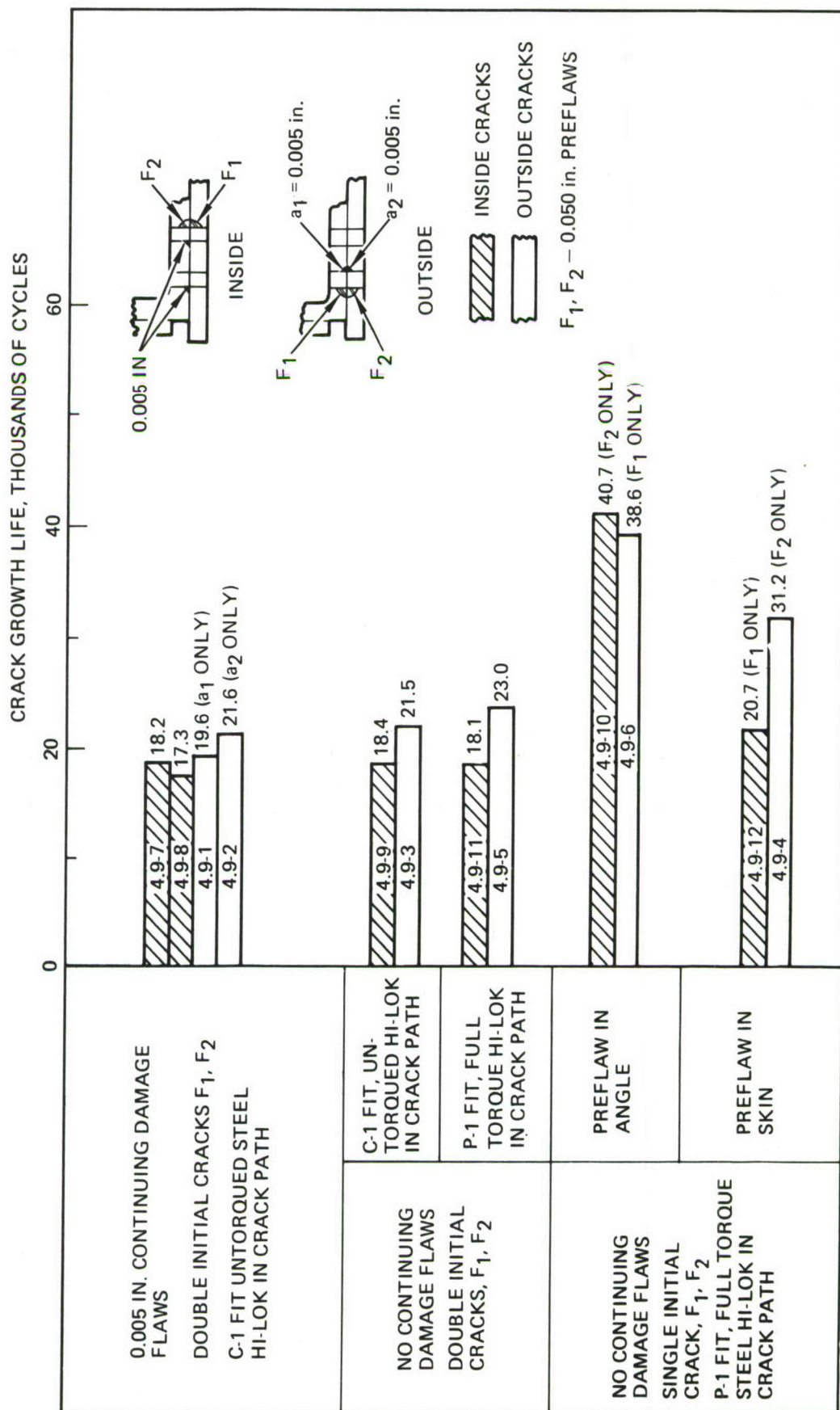
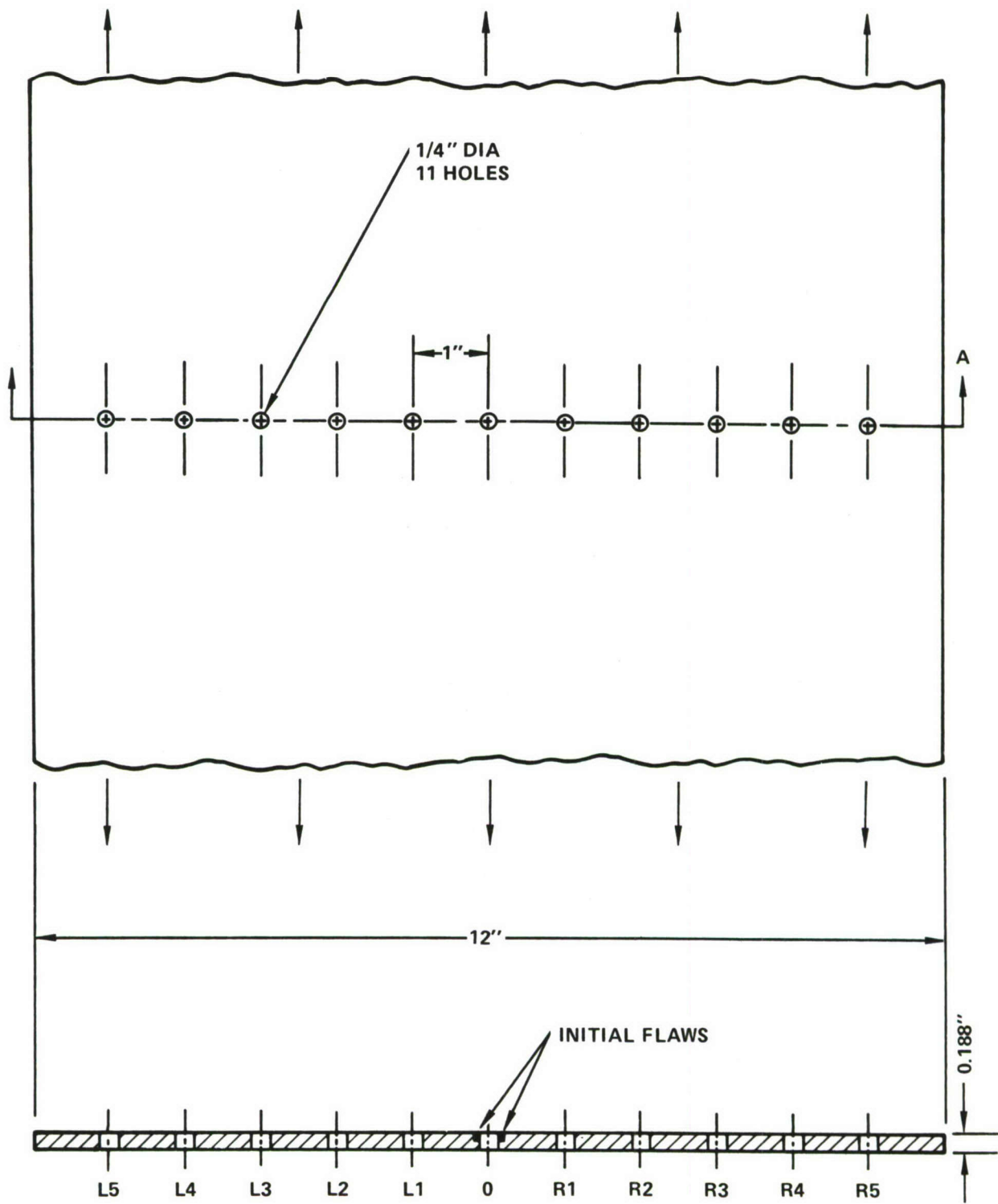


Figure 12. Comparison of Alternate Flaw Locations, Edge-Stiffened Specimens

Consider, for example, the hypothesis that lower stress levels would have magnified the effects of continuing damage flaws. Fatigue tests of the crack-growth-along-a-row-of-holes specimen, shown in Figure 13, run prior to the start of this program (Ref. 2), had long arrest times at each hole, creating the impression that continuing damage flaws (which would reduce this arrest time) would significantly shorten the total crack growth life. Such life reduction would occur even if the continuing damage flaws were not placed at the critical locations on the opposite side of the precracked hole. These tests were run at low cyclic stresses, ($R = 0.1$ and $S_{\max} = 10$ ksi or 13.8 ksi). Analyses of this specimen for $R = 0.1$ and $S_{\max} = 12$ ksi and 20 ksi are shown in Figure 14. As the figure shows, the continuing damage flaws are estimated to have more impact on crack growth life at 12 ksi than at 20 ksi.

A comparison between the predicted and total test lives for the Phase I joint specimens is shown in Figure 15. The following observations are made based on the correlations between those predicted and test results:

- The experimental growth rates of corner flaws for the double lap joint specimens are slower than predicted.
- For unclamped joints with clearance fit fasteners, the growth rate of a long through-thickness crack is accurately predicted except in Specimen 4.6A-3, where the entire crack growth history (corner crack and through-thickness crack) is much slower than in replicate Specimen 4.6A-4. The cracks grew slightly faster than predicted in Specimen 4.6A-2 but the acceleration was caused by the presence of secondary cracks.
- Growth rates of corner flaws and through-thickness cracks in the double lap joints are slower in fully-clamped joints with interference-fit fasteners than in unclamped joints with clearance-fit fasteners, and slower than the predicted rates by factors of about 2 to 4. The larger factors obtained in Figure 15 were due to arrestment of the crack growth at fastener holes.
- The predictions for the single-lap joint specimens tend to be unconservative, overestimating crack growth lives by a factor of roughly 1.5. The most likely explanation is that the transverse bending stresses have been ignored in the predictions. The results of strain gage measurements indicated that transverse bending increased the peak tension stress by about 40 percent in the skin at the faying surface. A uniform 40 percent stress increase would increase the crack growth rates by a factor of approximately 3.0. If this bending stress were accounted for in this manner in the analysis, the growth rates would be overestimated, as they were for the double lap joints.



SECTION A-A

Figure 13. Specimen for Crack Growth Between Holes (Ref. 2)

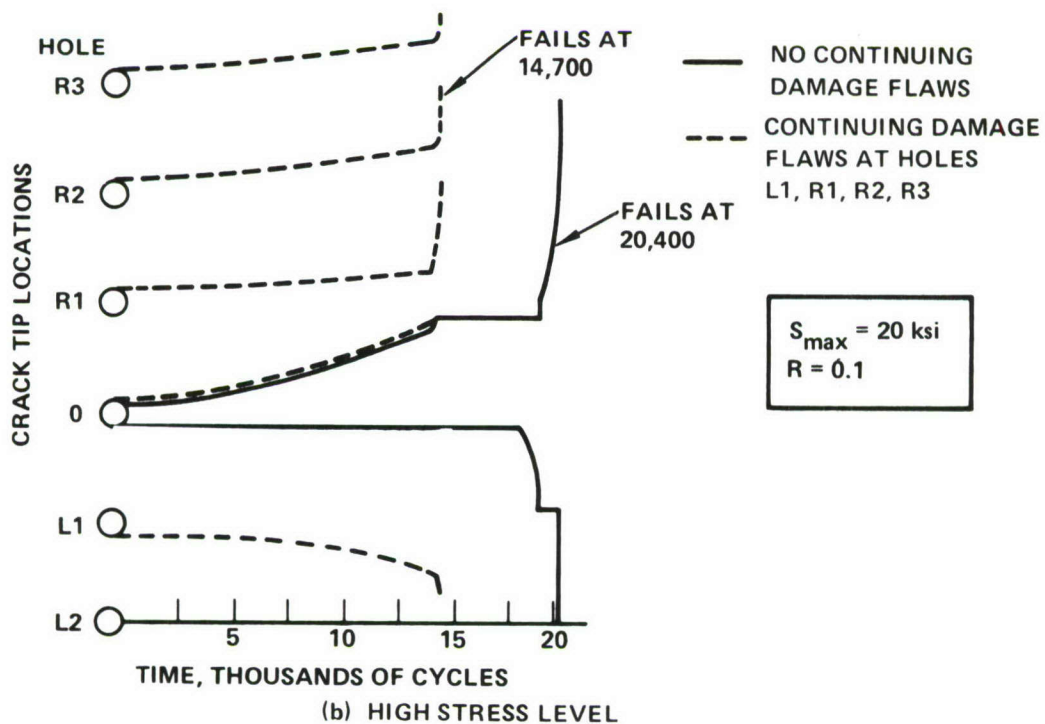
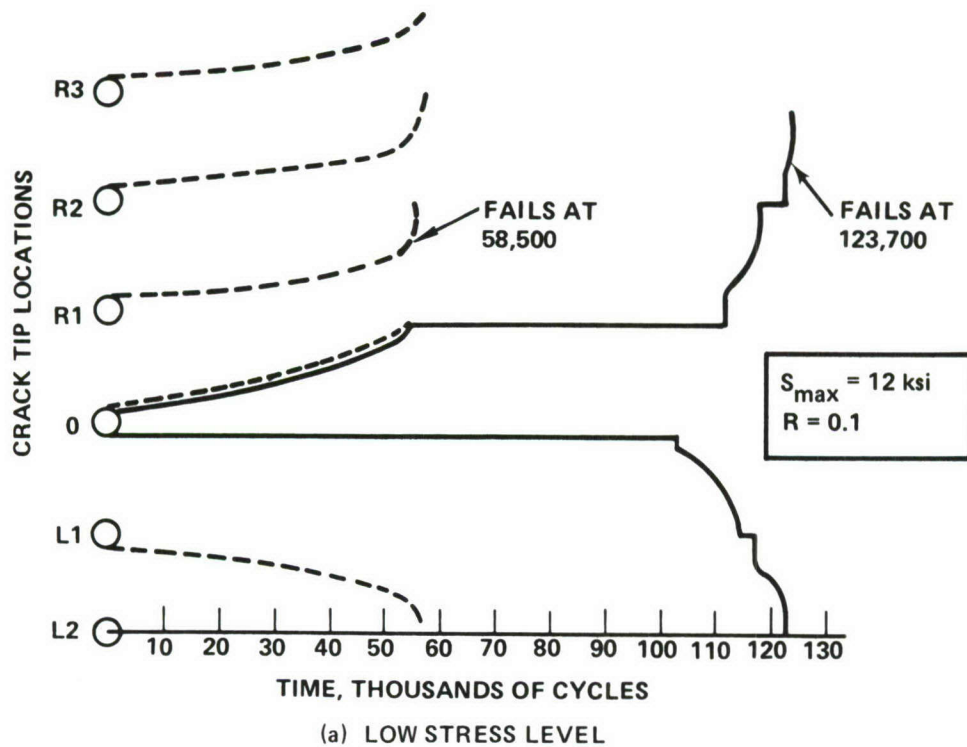


Figure 14. Analytical Crack Growth Predictions, Hole-to-Hole Specimen

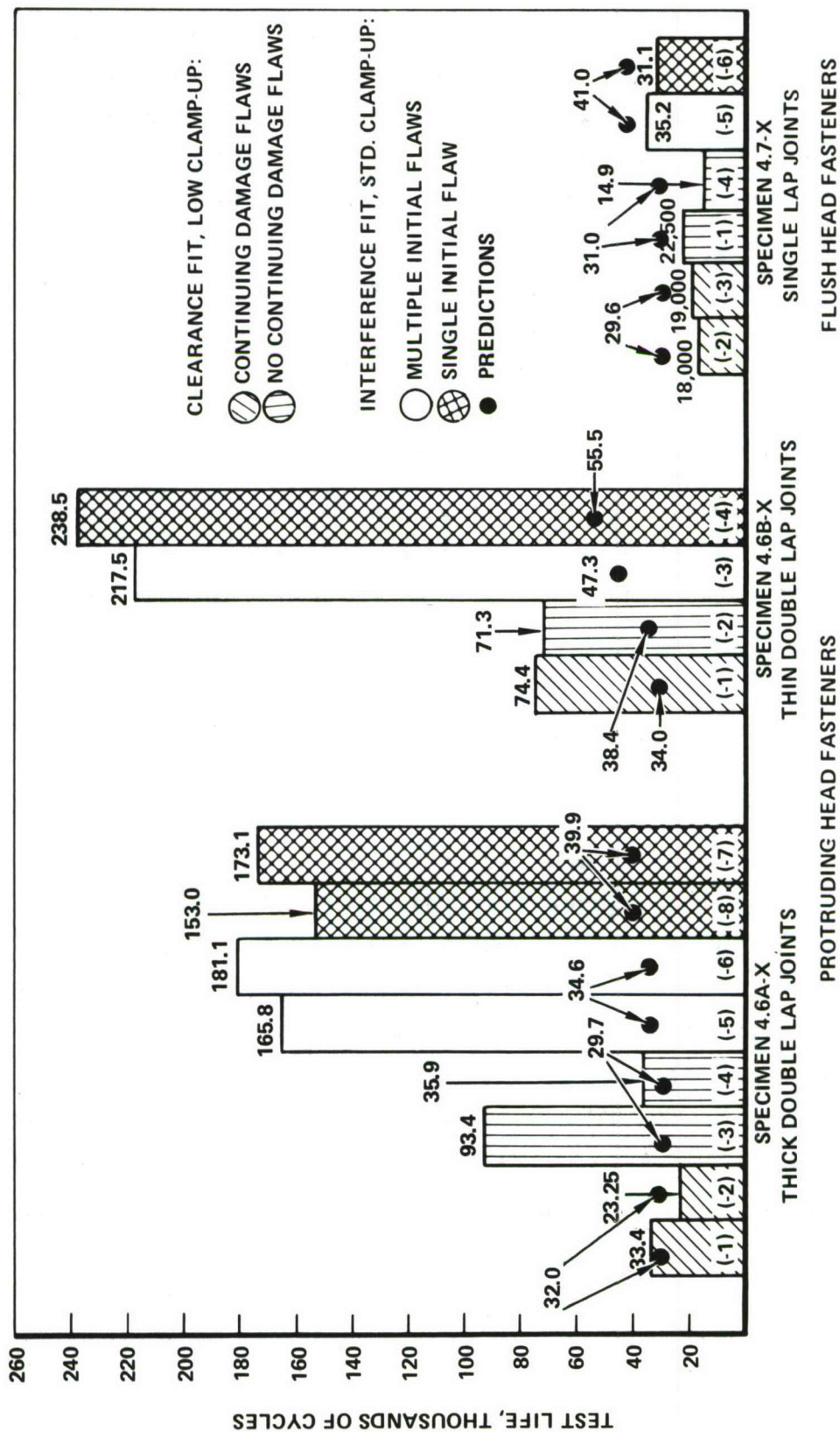


Figure 15. Predicted and Test Lives for Precracked Single-Lap and Double-Lap Joint Specimens

The greatest error in predictions was in estimating crack arrest periods for the double lap joints. Figure 16 compares predicted and actual crack arrest periods at the interference-fit fully-torqued fasteners in the immediate path of the preflaw. The crack arrest period is defined as the number of cycles from the time of crack arrest at the hole until reinitiation on the opposite side of the hole or, if the crack does not reinitiate, until specimen failure. In most of the double lap joint cases the crack did not reinitiate and failure occurred by fretting nearby. The predictions were based on baseline data which inadvertently had teflon tape applied across the entire faying surface. Thus these baseline test results failed to adequately reflect the life-extending benefits of faying surface friction for a nonlubricated joint.

Long crack arrest periods were not always observed, as seen in Figure 16. The crack arrest periods are very long for the double-lap joint specimens with protruding head fasteners but very brief for the single lap joint specimens with flush head fasteners.

An appropriate series of supplementary baseline fatigue tests was conducted to measure the crack-arrest capability of a fully-torqued Hi-Lok fastener. These tests are summarized in Table 3. The modified compact tension specimen with $W = 5.0$ inches was used. In Specimens N-1, N-2, A, B, and C, the 0.25-inch diameter hole was at the end of the slot and a fully-torqued clearance fit fastener was inserted in the hole. In specimens D, E, and F, a ligament of material of length $b_e = 0.25$ inch was left between the end of the slot and the edge of the hole, and a fully-torqued interference-fit fastener was inserted in the hole. (The 0.25 inch ligament broke after a few hundred cycles, which were not included in the tabulated crack initiation times.) In specimens B through F a square washer $1 \times 1 \times 0.182$ inch was used to simulate the fastening of a cracked member to an uncracked member.

The test results are shown in the last column of Table 3. The presence of the fully-torqued fastener improved the fatigue life significantly in all cases (by factors ranging from 2.0 to 36.2). Of all tests with fasteners, Specimen C with a flush-head clearance-fit fastener had the shortest life,

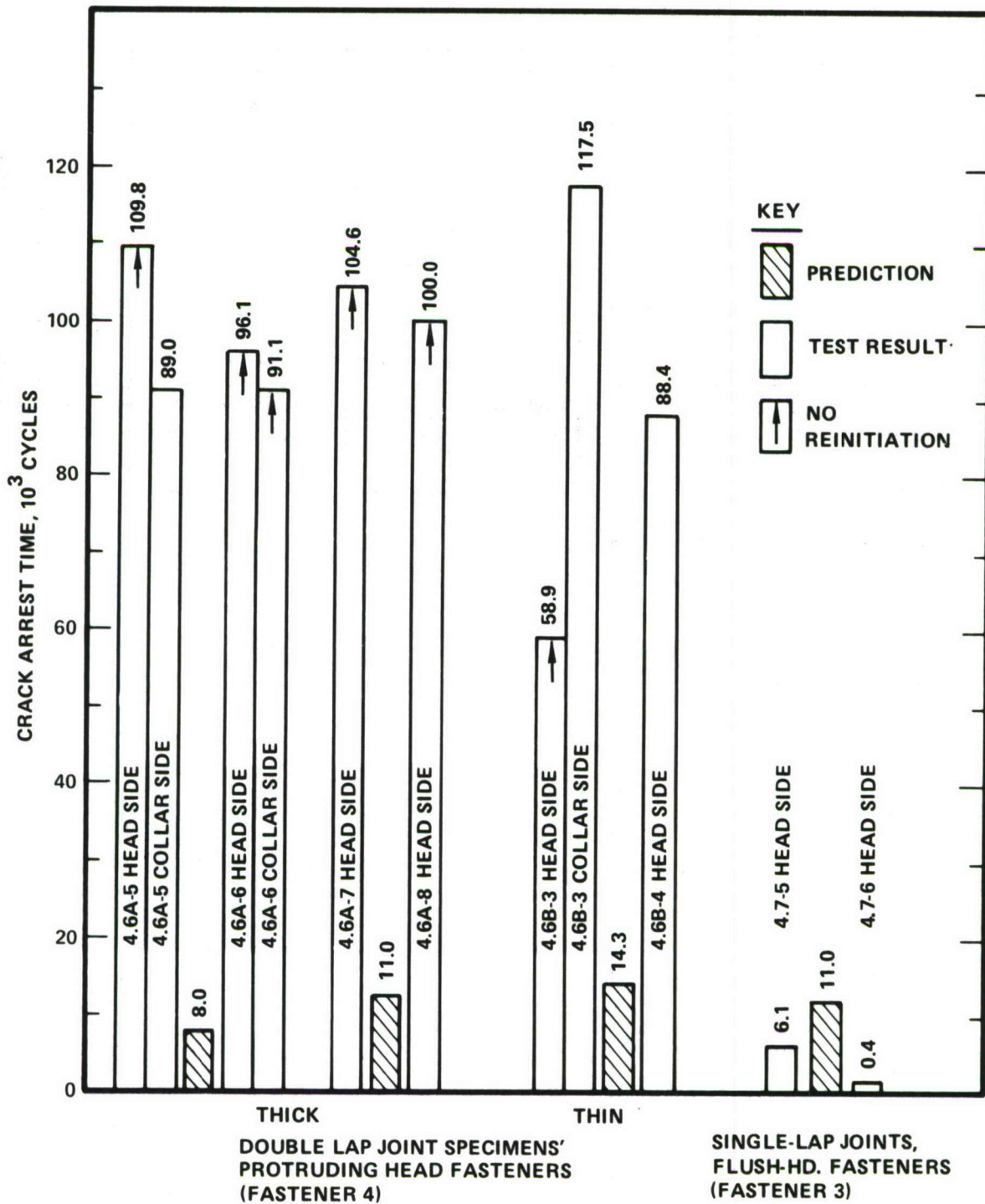


Figure 16. Comparison of Arrest Times at the Torqued, Interference-Fit Fastener in the Precrack Path

TABLE 3. MODIFIED COMPACT TENSION SPECIMEN FATIGUE TESTS

Specimen Number	Fastener Fit			Side of Fastener Contacting Specimen			b_e (Inches)	1 x 1 In. Washer Used	Fatigue Life (Cycles)
	Open Hole	Clear. Fit	Inter. Fit	Flush Head	Protrud. Head	Aluminum Collar			
N-1	x						0	No	7,570
N-2	x						0	No	8,671
A		x			x	x	0	No	49,253
B		x			x		0	Yes	292,910
C		x					0	Yes	16,580
D			x	x			.25	Yes	140,160
E			x	x		x	.25	Yes	64,650
F			x		x		.25	Yes	227,760

$$\frac{P_{\max}}{B} = 8665 \frac{\text{lb}}{\text{in}}$$

$$k_t^S \max = 113.4 \text{ ksi}$$

$$R = 0.1$$

Fasteners Used:

HL50-8-3
HL50-8-6
HL51-8-6

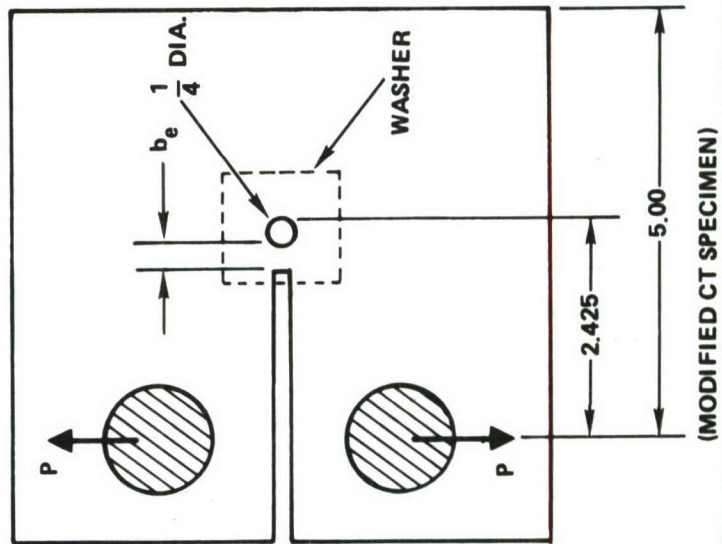
Collars:

HL90LP-8

Washer: 1 x 1 x 0.182 inch

7075-T6 Aluminum

Spec. Thickness $B = 0.182$ inch



16,500 cycles. However, this result may be misleading due to the fact that b_e was zero. The reason for having b_e equal to 0.25 inch in specimens D, E and F was to allow the fastener interference to be developed properly. However with b_e equal to zero, the tapered head of the fastener in specimen C would simply spread the hole upon installation in a manner unlike anything actually seen on the structure, thus significantly affecting the reliability of the specimen C result. Specimen D with an interference-fit flush-head fastener had a substantially longer life, 140,160 cycles.

These test results substantiate that friction under the head of a torqued fastener is responsible for significant extensions in crack initiation time when a crack arrests at the fastener hole. However, there are insufficient data from these 6 tests to confidently identify consistent differences in the crack-arrest capabilities of protruding heads, flush heads and aluminum collars.

It seemed significant in view of the short crack reinitiation times and test lives of the single lap joints compared to the double lap joints that the single lap joints had flush-head fasteners. The comparisons appear to show some superiority of the protruding head fastener. However, the flush-head fastener seems capable of some degree of crack arrestment by friction beneath the head. The significance of fastener head type was further investigated by testing single lap joints during Phase II.

The crack arrestment capability of fasteners was used in the testing of the stringer-reinforced specimens. In 19 of these specimens the skin crack growing away from the stringer began growing at a high fatigue rate. It was desired to postpone instability of this crack and allow time for secondary damage to initiate and grow in the region near the stringer. Therefore, the skin crack was stop drilled and a fully-torqued 0.375 inch clearance-fit protruding-head steel Hi-lok fastener was inserted in the hole. (A stack of steel washers was used between the collar and the specimen surface because the shank length of the shortest available 0.375 diameter Hi-lok was more than the sheet thickness.) In all 19 cases the crack was arrested very effectively by this procedure.

Figure 17 summarizes the crack growth lives and predictions for the edge stringer specimens. The initial damage conditions are shown for each specimen, and the predicted crack growth lives are compared to the test lives. In the tests, specimen failure always occurred soon after one member failed. This agreed with the preselected failure criterion for the prediction: When one member fails the specimen fails.

All eight specimens with initial cracks in both the angle and the skin had nearly identical crack growth lives, ranging from 17,300 cycles for Specimen 4.9-8 to 23,000 cycles for Specimen 4.9-5. Among those eight the most significant variable was initial crack location. Lives for the four specimens with outside initial cracks in both members ranged from 19,600 cycles to 23,000 cycles, whereas test lives for the four specimens with inside initial cracks in both members ranged from 17,300 to 18,400 cycles. For the outside initial cracks, the presence of continuing damage flaws seemed to have little or no effect, whereas the interference and torque on the secondary fastener (F2) in the crack plane seemed to have a slight beneficial effect. Neither continuing damage flaws nor torque and interference on the secondary fastener appeared to significantly affect the crack growth life for specimens with double inside initial cracks.

Specimens with an initial crack in just the angle or just the skin lasted longer than specimens with initial cracks in both the angle and the skin. This life extension resulted from the natural transfer of load from the cracked member to the uncracked member, which slowed the growth rate of the crack. This occurred to some extent in all four specimens with single initial cracks. However, the resulting life extension was small in Specimen 4.9-12 because the inside skin crack grew out of the region of influence of the angle (necessitating stop drilling) before the load transfer from the skin to the angle became very large.

Except for Specimens 4.9-11 and 4.9-12, all of the predicted crack growth lives were within a factor of 1.33 of the actual test lives. In making these predictions, no effort was made to account for load shedding from cracked to less-cracked members. Of course, accounting for load shedding could make predictions farther off in some cases.

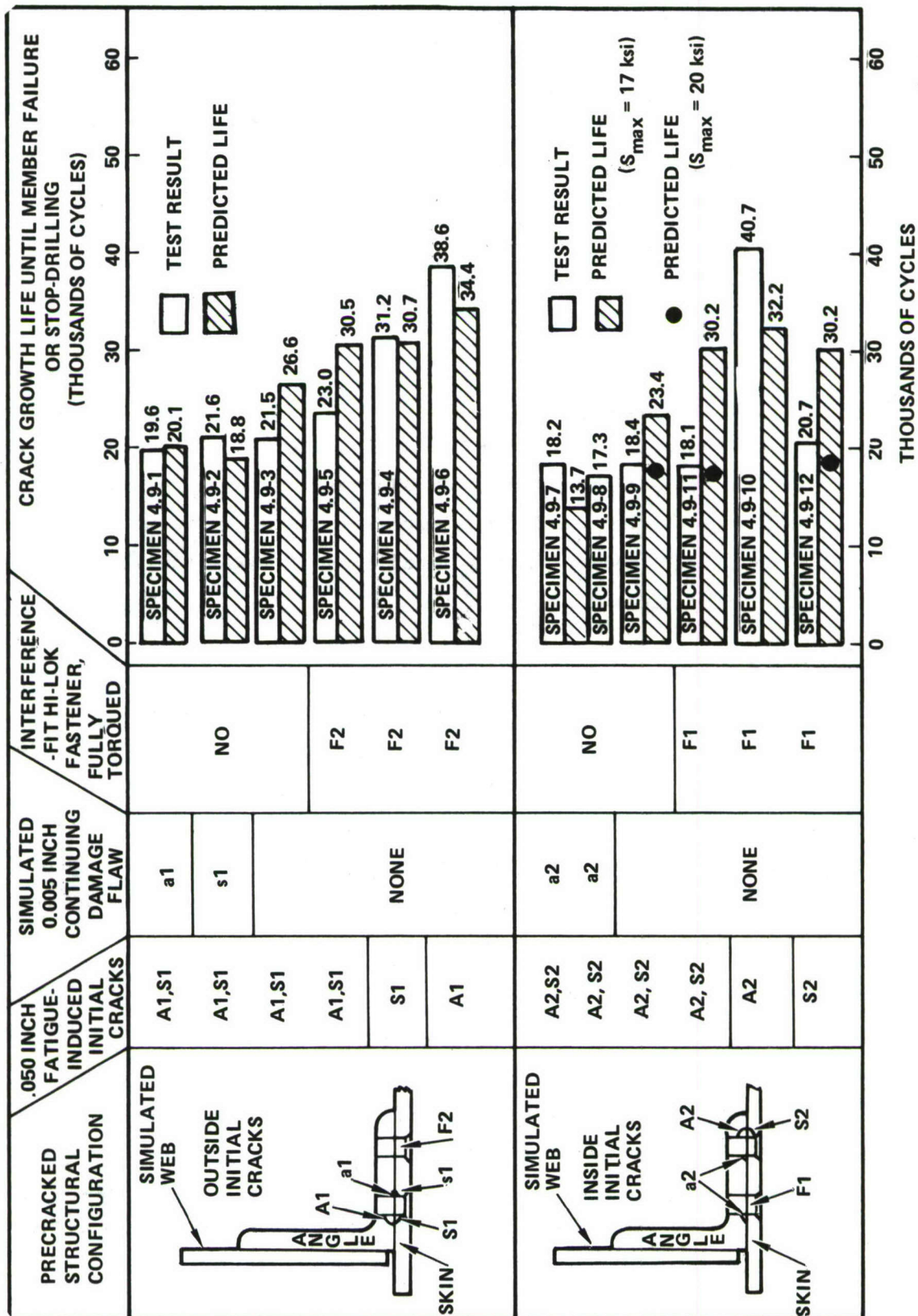


Figure 17. Summary of Crack Growth Lives for Edge-Stringer Reinforced Specimens

The somewhat larger error in the predictions for Specimen 4.9-11 and -12 is caused by underestimating the growth rate of the inside crack in the skin. Based on strain gage readings, the stress was estimated to be approximately 20 ksi rather than 17 ksi in the vicinity of the inside crack in the skin. These increased stresses are applicable to Specimens 4.9-7, -8, -9, -11 and -12. The life predictions for Specimens 4.9-7 and -8 are unaffected because, with continuing damage flaws in the angle, the angle is theoretically the first member to fail. However, the life predictions for Specimens 4.9-9, -11 and -12 are improved. The improved estimates are 18,000, 17,700 and 17,900 cycles as shown in Figure 22.

The outside crack in the angle consistently grew faster than predicted. A number of possible sources of error in the analysis exists which could affect the predicted results to be either longer or shorter. However, despite these possible sources of error, the predictions were well within a factor of 2 of the test results on all 12 tests. Similar predictability was achieved on the 24 specimens with central tee stringers.

2. PHASE II RESULTS

Baseline spectrum fatigue and crack growth test results are plotted in Figures 18 and 19 along with predictions. The X-symbols in these two figures denote earlier data for the same spectrum loading sequence, obtained on a different batch of 0.188 inch-thick 7075-T6 sheet material. These earlier data were obtained on 6-inch-wide center-hole specimens. In plotting these earlier data, a neat-fit aluminum pin in the center hole was assumed not to affect the k_t or stress intensity factor.

Predictions were made by using the baseline constant-amplitude data and first assuming no load-interaction effects; then assuming a modified Willenborg-type retardation model. Because of the short periodicity of the loading sequence, the estimated size of the overload-affected zone increases linearly with the square of reference stress intensity K_{Ref} . As a consequence, for each stress cycle in the spectrum, the corresponding values of the Willenborg effective peak stresses $S_{eff(max)}$ and $S_{eff(min)}$ are the same throughout the life and are closely approximated by

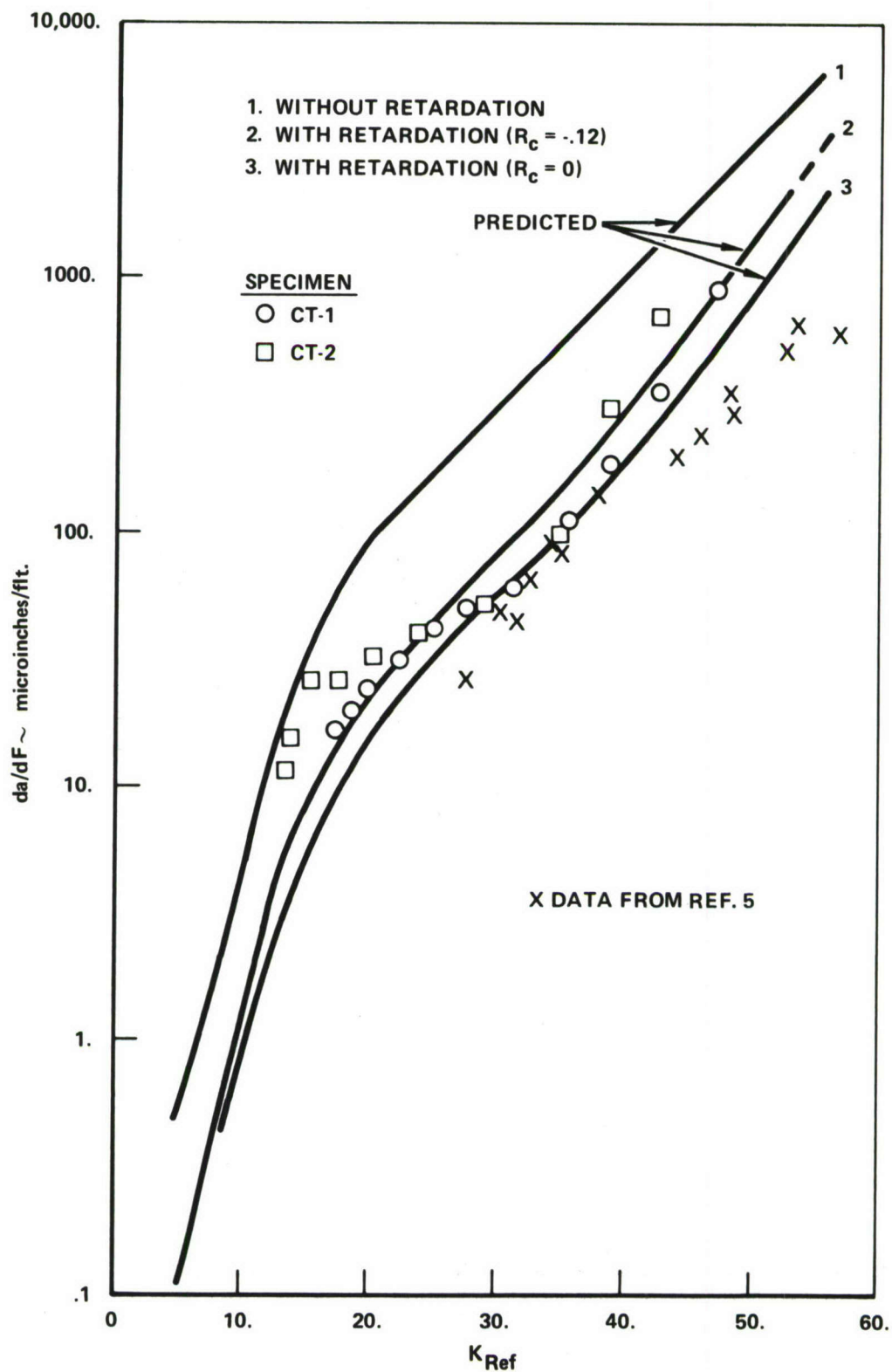


Figure 18. Baseline Spectrum Crack Growth Rates for the 80-Flight Loading Sequence

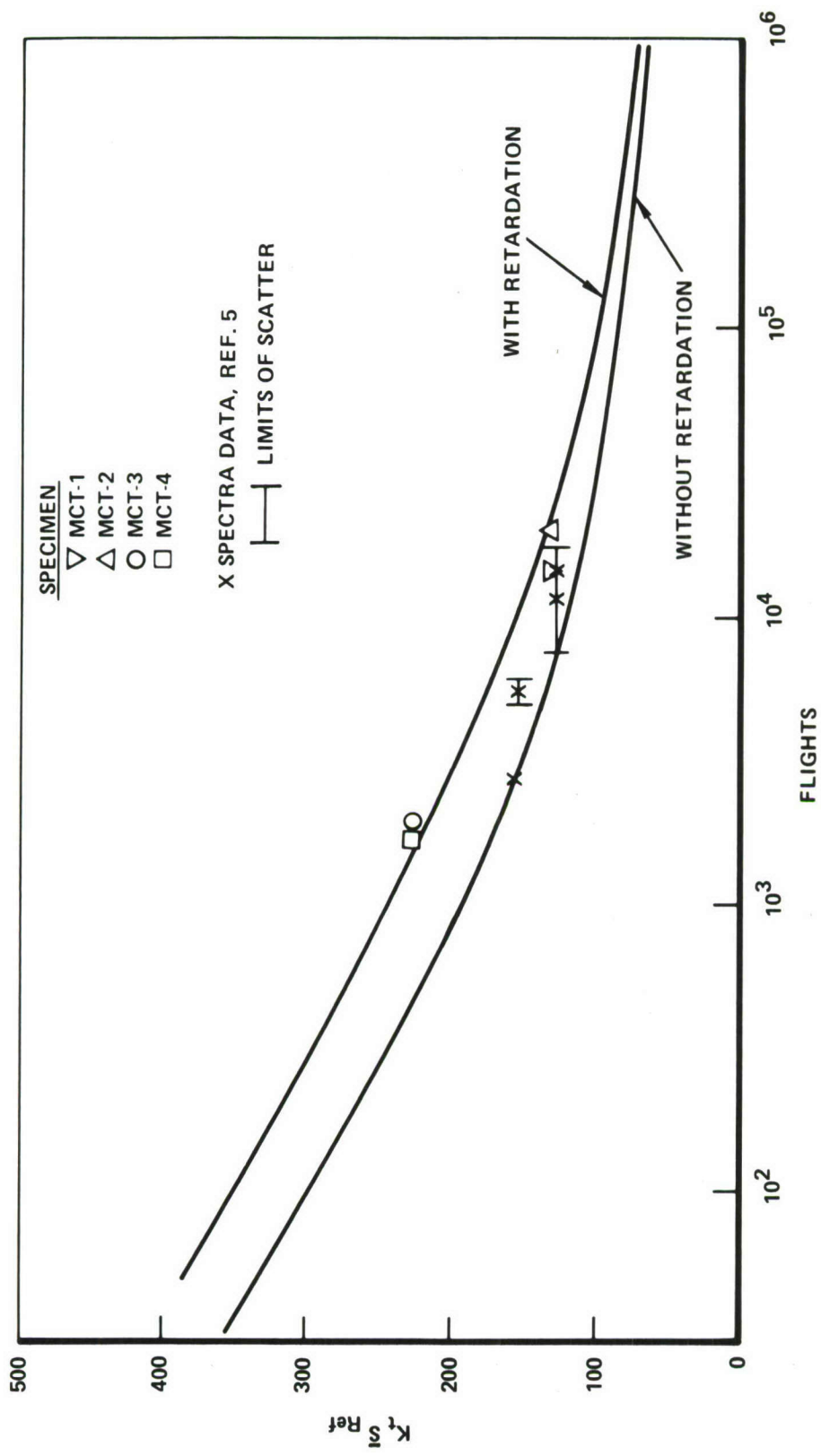


Figure 19. Baseline Spectrum Crack Initiation Lives for the 80-Flight Loading Sequence

$$S_{\text{eff}}(\text{max}) = \text{MAX} [0, 2S_{\text{max}} - S_{\text{Ref}}] \quad (2a)$$

$$S_{\text{eff}}(\text{min}) = \text{MAX} [R_c S_{\text{eff}}(\text{max}), S_{\text{max}} - S_{\text{Ref}}] \quad (2b)$$

The spectrum computations require that the baseline constant-amplitude data, all obtained at $R = 0.1$, be generalized for all stress ratios. To accomplish this, Walker (Reference 6) uses the single parameter $\overline{\Delta S}_{\text{eff}}$, where

$$\overline{\Delta S}_{\text{eff}} = S_{\text{eff}}(\text{max}) [1 - S_{\text{eff}}(\text{min})/S_{\text{eff}}(\text{max})]^m \quad (3)$$

For aluminum, $m = 0.5$. Data have shown that equal values of $\overline{\Delta S}_{\text{eff}}$ cause equal constant-amplitude crack growth rates regardless of stress ratio.

Prediction Number 1 in Figure 18 is obtained by assuming no retardation effects. The effective maximum and minimum stresses are set equal to the actual applied stresses for all cycles in the spectrum. Predictions 2 and 3 in Figure 18 are obtained by assuming retardation effects and employing Equations (2) to compute the effective maximum and minimum stresses, using $R_c = -0.12$ and 0, respectively.

Since Equations (2) and (3) deal strictly with stresses and contain no crack length parameter, it is possible to use these equations in the estimation of crack initiation lives due to spectrum loading. The computation method is identical to Miner's Rule.

The computation of crack initiation time was done both without retardation (assuming that the effective maximum and minimum stresses are equal to their actual applied values), which is Miner's Rule, and with retardation (using Equations (2) with $R_c = -0.12$). The results are plotted in Figure 19.

This is probably the first time that the Willenborg retardation model has been applied to predict spectrum fatigue crack initiation. No theoretical basis for using it is offered here, except that it has been empirically observed that the occurrence of an overload will delay crack initiation, just as it will slow the growth of a crack. Comparison in Figure 19 between the

crack initiation data on Specimens MCT-1 through MTC-4 and the corresponding retardation prediction is interesting.

Figure 20 shows the effect of fastener head type on the crack growth life for the constant amplitude tested single lap joint specimens. The specimens with protruding-head fasteners had slower crack growth rates and longer crack reinitiation times than those with flush-head fasteners. The differences in crack reinitiation times (cross-hatched area in Figure 20), however, were not as striking as the reinitiation time differences between the single lap and double lap joints. The bending stresses that are essentially absent in double lap joints but present in the single lap joint specimens apparently had a substantial effect on these crack reinitiation times.

Results of the spectrum tests conducted on the single lap joints are summarized in Table 4.

The lives of specimens 4.7-11, 4.7-12, and 4.7-13 were nominally the same. This is in contradiction to the differences in the constant amplitude results, where the protruding head fasteners furnished slightly longer lives. Examination of the spectrum-tested specimens showed that in all four cases the cause of failure was fretting. Failure was not caused by the steady progression of the initial fatigue crack but rather by the independent initiation and growth of several fretting cracks.

The conclusion from all tests is that the protruding head fasteners seem to offer a slight advantage with respect to fatigue crack reinitiation and propagation. However, the primary differences between the results of the single lap and double lap joint tests of Phase I were due to bending. Moreover, if failure is caused primarily by fretting at the faying surface, little if any advantage can be gained by using protruding head fasteners. It should be pointed out that the differences shown between the flush head and protruding head constant-amplitude test results (4.7-5, 4.7-6, 4.7-7, 4.7-8) are on the order of what could be predicted by considering the increase in net section stress caused by the countersink for the flush head fasteners.

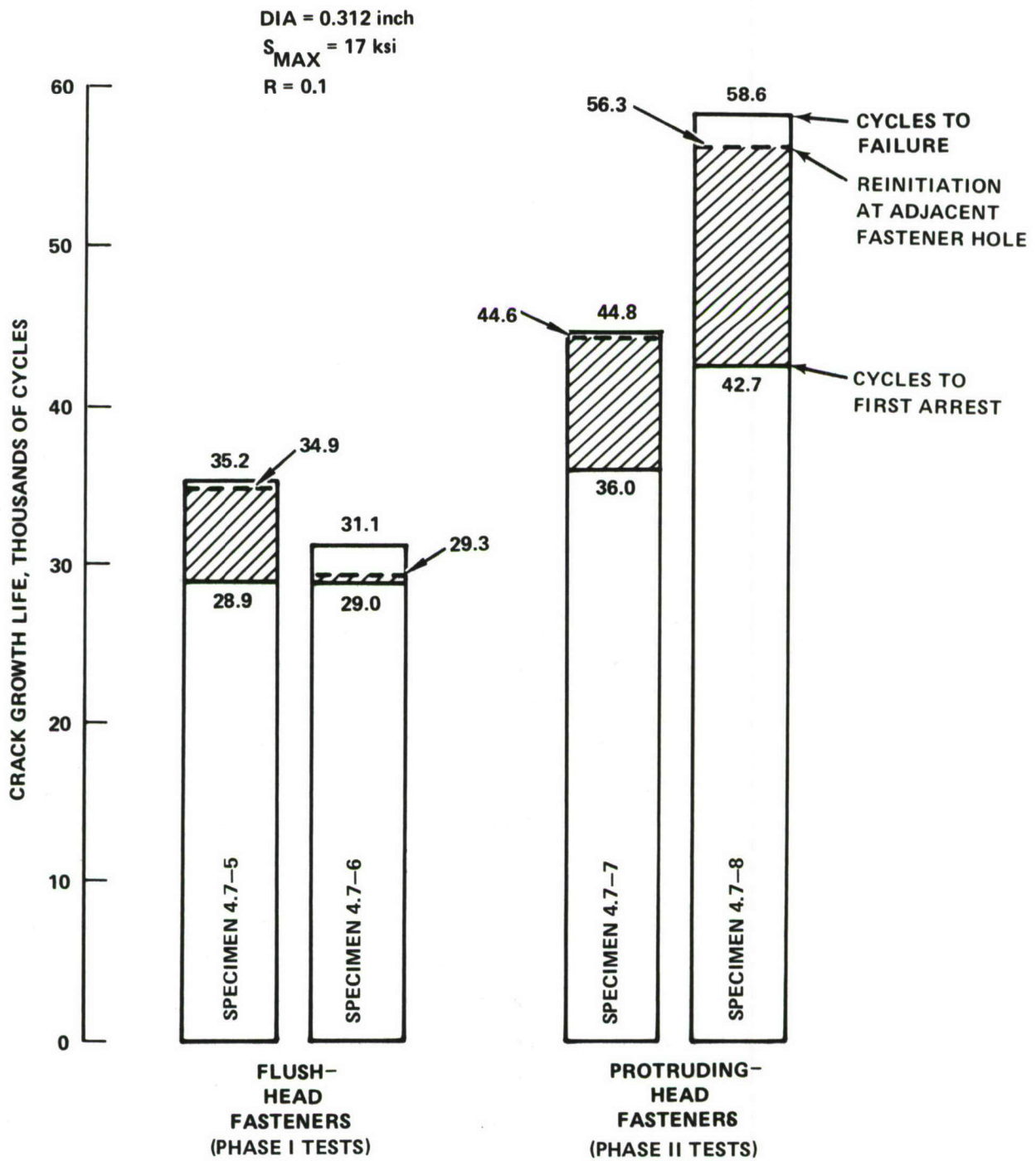


Figure 20. Effect of Fastener Head Type in Constant Amplitude Tests of the Single-Lap Joint Specimen

TABLE 4. SPECTRUM TESTS OF SINGLE LAP JOINT SPECIMENS
FOR EFFECT OF FASTENER HEAD TYPE

	80-Flight Spectrum		
	Spec. No.	S_{Ref} (ksi)	Flights To Failure
HL51-10 Flush- Head Hi-lok Fasteners	4.7-10	25	28,840
	4.7-11	30	18,119
HL50-10 Protruding- Head Hi-lok Fasteners	4.7-12	30	20,440
	4.7-13	30	17,870

For all spectrum tests of joints and split skin tee specimens, there were prior constant amplitude test results for the same configuration. The equivalent k_t and equivalent stress intensity factor methods, described in Volume I, were used to predict the crack growth lives based on the results from the constant amplitude tests. As seen in Figure 21, results from these two first-order prediction methods are within about a factor of 2.0 of the test results. This agreement is achieved despite the greater tendency toward fretting in the single lap joints when subjected to spectrum loading. The methods would be expected to break down when a change in failure mechanism occurs.

The fracture surface of a typical specimen contains characteristic markings that can be related to the spectrum loading sequence. The largest tensile loading in the 80-simulated-flight periodic sequence, which occurs in the 39th flight, causes the crack front to jump ahead, especially at mid-thickness. Dark gray areas or bands on the fracture surface show the length of each such jump. Thin silvery bands separating them indicate fatigue crack growth during the other (smaller) 1079 cycles that recur each 80 simulated flights.

Therefore, the crack growth rates, and in fact the entire crack growth history, can be identified by counting or measuring the spacing of these fracture surface markings. From the markings it was possible to determine the extent of cracking in the various members and identify the shape of the crack.

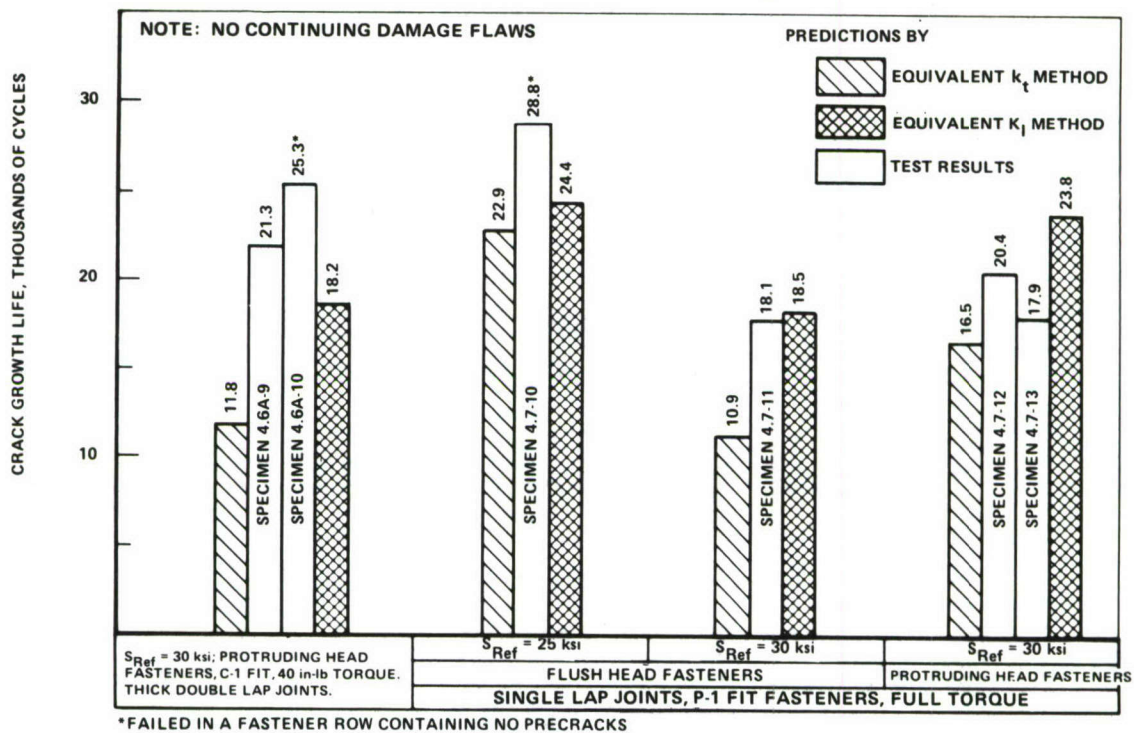


Figure 21a. Spectrum Test Lives and Life Predictions for Joints

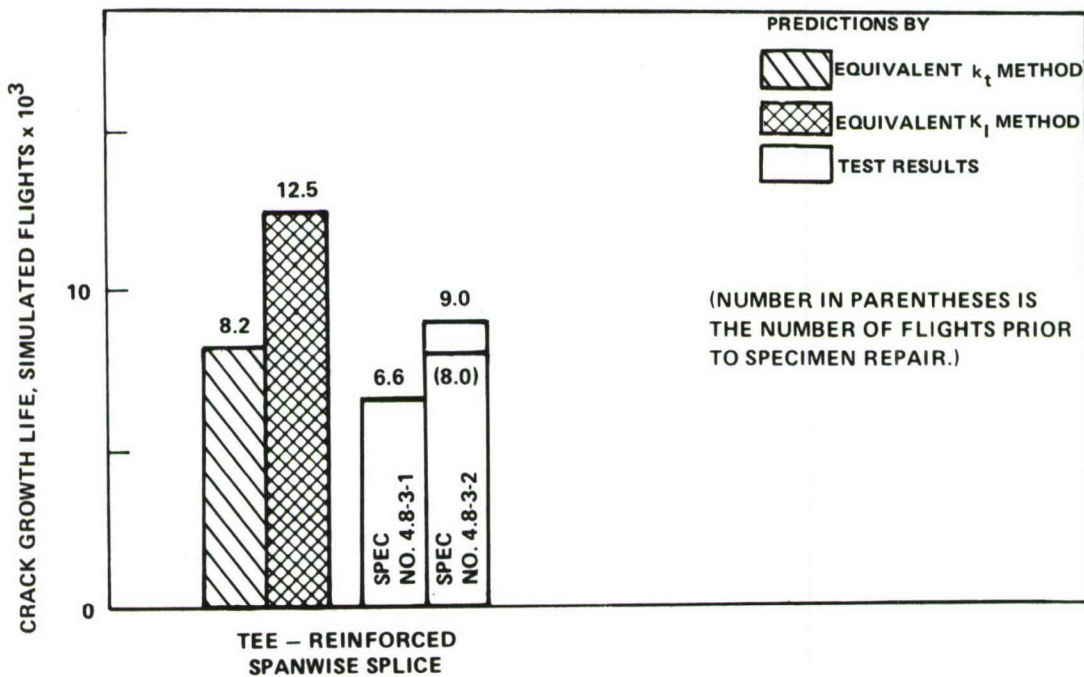


Figure 21b. Spectrum Test Lives and Life Predictions for Tee-Reinforced Split-Skin Specimens

In the constant amplitude tests, the crack front shape is almost perfectly circular in the region of the tee. The difference in crack front shape between the constant amplitude and spectrum specimens occurs because crack front tunneling is more prevalent at the higher maximum stress level (30 ksi versus 17 ksi) used in the spectrum tests.

Four two-bay specimens (Table 2) were precracked and constant amplitude tested at two stress levels to verify that crack growth patterns for the center stringer and edge stringer specimens extrapolate to multiple stringer structure and to other stress levels.

Specimens 4.10-3 and 4.10-4 were nominally identical, with 0.050-inch inside corner cracks in the angle and (at the same holes) the skin. Figure 22 is a plot of crack size versus time, with the time scale normalized by the number of cycles to failure. Thus, differences between the plots for the two specimens indicate different relative time periods for the various crack initiation and crack growth segments which sequentially combine to cause the final failure.

To understand the difference observed, consider the damage condition when 90 percent of the life has been consumed. Since failure occurs rapidly thereafter, this damage condition can be considered for practical purposes to be a critical (pre-failure) condition. For specimen 4.10-3 this damage is more extensive, because the applied stress is lower. To achieve this damage condition, the cracks in Specimen 4.10-3 had to reach other lengths earlier than the cracks in 4.10-4.

Thus the differences observed are exactly what would be expected to result from a stress level change. This is an important observation, since all specimens in this program were run at one stress level, 17 ksi. This comparison suggests that phenomena observed in the stringer reinforced tests run at 17 ksi would also be expected at different stress levels. This is further supported by comparing in detail the crack paths for these two specimens, which are almost identical.

It should be noted that as the crack grew across each specimen from member to member, the crack plane shifted from one fastener hole to one

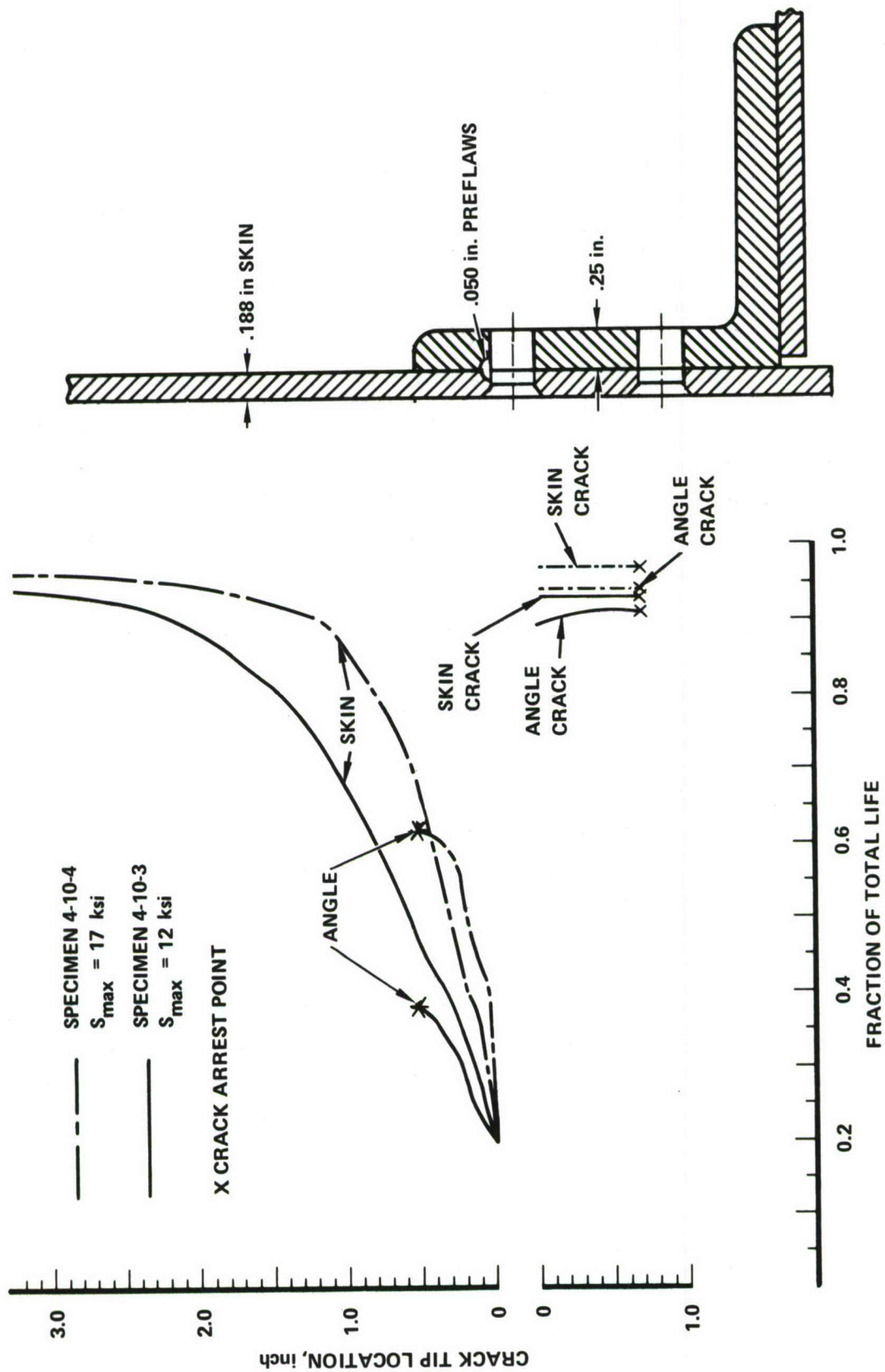


Figure 22. Stress Level Effect, Two-Bay Specimen with Pre-cracked Edge Stringer and Skin

immediately above or below. This shifting is expected in parallel-load-path structure because the stress severity factor is maximum at the location one fastener hole from the crack plane, where load is transferred from the cracked member. Finger-tight, clearance-fit fasteners were used in all two-bay specimens all the way across the plane of the precrack. All other fasteners (including those one fastener hole from the crack plane) were interference fit, fully torqued. Nevertheless, the crack plane shifted in Specimens 4.10-3 and 4.10-4 to a plane of these torqued, interference-fit fasteners.

Specimens 4.10-1 and 4.10-2 were also initially identical, with 0.050-inch outside corner flaws located at the faying surface between the central tee and one sheet at the same fastener hole. These two specimens, tested at two different stress levels, show the same trend of differences as Specimens 4.10-3 and 4.10-4, due to the longer critical crack length for the lower stress level.

Another purpose of testing the two-bay stringer specimens was to see whether the added structural complexity would result in significant differences in crack growth behavior. This assessment was accomplished by comparing test data from Specimens 4.10-2 and 4.10-4, which were tested at $S_{max} = 17$ ksi, to corresponding center stringer or edge stringer specimens previously tested at $S_{max} = 17$ ksi. Tee-reinforced split-skin Specimens 4.8-3-7 and 4.8-3-8 were comparable to Specimen 4.10.2. All three had double initial outside cracks in the tee and skin, no continuing damage, and all fasteners on the crack line installed with a clearance fit and low fastener torque.

It was found that the added structural complexities did not significantly alter the early crack growth rates. The growth of the initial skin cracks for all three specimens accelerated rapidly after the initiation of a new skin crack on the opposite side of the initial cracks.

The early crack growth histories were compared for two-bay Specimen 4.10-4 and edge-stringer Specimen 4.9-9. Both had double initial inside cracks in the angle and skin, no continuing damage flaws, and clearance fit fasteners with low fastener torque in the plane of the precrack. The secondary cracks initiated

4000 cycles earlier and the growth rates of the initial cracks were slightly faster in the two-bay specimen than in Specimen 4.9-9. However, these differences were small, and it appears that no significant changes in crack growth result from the added structural complexity of the two-bay specimen.

SECTION V

CONCLUSIONS AND RECOMMENDATIONS

The following observations and conclusions result from the testing and analysis of the precracked joint specimens:

- Fastener torque and faying surface friction effects in an unsealed joint can lead to long crack growth lives and shift the failure mechanism from failure by progressive cracking across the fastener holes to failure due to fretting cracks. Faying surface sealant (Reference 4) seems to protect small cracks against environmental attack but compromises the beneficial effects of faying surface friction. Analytical methods are not currently available to account for the effect of fastener torque and faying surface friction.
- If there are high bending stresses, there is an increased tendency for multiple cracks to initiate at the fastener holes. For example, while the central fastener in Row 1 of the skin contained the pre-crack in single lap joint specimen 4.7-10, failure occurred in the doubler across Row 2 by the coalescence of 14 cracks, one on each side of all seven holes in the failed row.

Similarly, when the fasteners are not fully torqued in the double lap joints the crack initiation time at the holes becomes less than the growth time from hole to hole. For example, at $S_{\max} = 17$ ksi, $R = 0.1$ and low fastener torque, there was little difference between test lives for double lap joint specimens with or without continuing damage flaws because of such multiple crack initiations.

For both of these cases, the initial flaw condition was unimportant, because failure occurred due to independent cracks at several fastener holes.

- Friction under the head or collar of the fully-torqued fastener helps to retard the reinitiation of the crack. Faying surface friction also has a role in postponing reinitiation. Occasionally the collar can crack, allowing the cyclic tensile deformations that lead to reinitiation.

- Spectrum loading was observed to have three possible effects:
 - Caused more of a tendency toward fretting cracks near the holes in single lap joints.
 - Had a predictably shorter critical crack size due to a spectrum maximum stress of 30 ksi compared to a constant amplitude maximum stress of 17 ksi.
 - Had a fairly predictable crack growth life, based on the complementary constant amplitude test result, even when the failure mechanism was different from that anticipated.
- Standard prediction techniques were accurate within about a factor of two for joints, except in dry (unsealed) fully-clamped joints without much transverse bending where faying surface friction and fastener head friction must be accounted for. When bending is present, it seems to accelerate both crack initiation and growth. From Reference 4, compression - tension loading of a double-lap joint can apparently be accounted for using the effective stress concept, Equation (3).
- Scatter in these tests was reasonably low, except for replicate specimens 4.6A-3 (93,400 cycles to failure), 4.6A-4 (35,900), and specimen 4.6A-12 (54,700). (Specimen 4.6A-12 was fabricated and tested later for Reference 4). When speaking of scatter, it is important to emphasize that some of the controls on machining and assembly of these specimens were more stringent than the controls normally used in machining and assembly of aircraft structure. Also, except for Specimen 4.6A-12, each pair of replicate specimens was precracked, machined and assembled at about the same time and on the same setup. Therefore it would be wrong to assume that the scatter in these tests is equal to the scatter of crack growth in aircraft structural joints.

The following observations and conclusions are made based on the analysis and testing of the stringer-reinforced panels:

- For stringer reinforced specimens with 0.050-inch corner precracks in both the stringer and sheet at a common fastener hole, the crack growth predictions were accurate within a factor of about 1.6 without considering load shedding from cracked to intact members. Predictions could be farther off if load shedding were accounted for. It should be kept in mind that the conditions for predicting were close to ideal. In making predictions for structure in service, where ideal conditions are not generally present and, in addition, the loads and environments are unknown and variable, the reliability of crack growth predictions could be substantially less than has been observed in this research program.

- The crack growth life is significantly reduced when a simulated 0.005-inch continuing damage flaw is present on the opposite side of the hole containing the initial 0.050-inch corner flaw. At $S_{\max} = 17$ ksi, $R = 0.1$, continuing damage flaws located at other locations had a negligible effect on life, although they did tend to grow as quarter-circular corner flaws.
- The lives of the split-skin tee reinforced specimens were shorter than the corresponding lives of the continuous-skin specimens. The split in the skin and the 0.062-inch increase in the fastener diameter slightly accelerated the crack growth process.
- Crack growth in the angle-shaped edge stringer tended to be somewhat faster than predicted. It appears that in-plane and transverse bending effects occur which were not considered in the analysis used.
- The practice of stop-drilling the skin crack proved to be an effective repair procedure for the stringer reinforced specimens when a fully torqued Hi-lok fastener was installed in the stop-drilled hole.
- Spectrum loading, using the 80-flight periodic loading sequence, marked the fracture surface so that the crack growth rates, crack front shape, and cracking sequence were clearly discernable on the fracture surface.
- Although the two-bay specimens introduced more structural complexity, the crack growth lives and cracking sequence were similar to the comparable center stringer and edge stringer specimens.
- Stress level had a predictable effect in the two-bay specimen. The critical crack length is shorter at the higher stress level so the growth of very short cracks encompasses a larger percentage of the crack growth life.
- In stringer reinforced structure, there can be a tendency for cracks to nucleate in an undamaged member one fastener hole away from the plane of cracking of the adjacent member, because the load transfer is maximum at that fastener hole. In some specimens, the crack was biased to remain in the plane of the precrack, the only place wherein all fasteners are low-torqued clearance-fit.
- Excluding cases with a continuing damage flaw and a primary crack on opposite sides of the same hole, variations in initial flaw multiplicity had little effect on early growth rates. However, single-crack specimens lasted longer because the crack had to initiate in the secondary member.
- When no continuing damage flaws were present, the first new flaws to initiate were on the opposite side of the hole containing the precracks. The initiation occurred especially fast if the precrack grew to a free edge, creating a deep edge notch. Fatigue crack initiation data can be used to predict the nucleation of these secondary cracks.

The specimen preparation and precracking procedures used in this program have been shown satisfactory for use in damage tolerance testing. These procedures are described in detail in Section VI of Volume I and are highlighted by the following:

- Prior to assembly, drill an undersized hole and mechanically notch the edge of the hole where a corner crack is desired.
- Cyclically load in bending or pin loading until a crack of predetermined size develops at the notch. Final crack growth rate for precracking was not high compared to the eventual initial crack growth rate in the test, to avoid initial retardation effects.
- Enlarge the hole to its final diameter, eliminating the mechanical notch and leaving a fatigue crack of desired size.
- Assemble the specimen, matching assembly procedures and details to that of production in a manner compatible with MIL-A-83444. The fastener at the initial flaw location was a noninterference fit fastener without beneficial clamping effects, to simulate the criteria and also so that the initial flaw could have its best chance to grow.
- Inspect thoroughly during the entire specimen preparation and precracking process, especially in the region where failure is anticipated, to help avoid the uncertainty and expense of trying to investigate anomalous test results afterwards.

Based upon the results obtained from this program, recommendations can be made pertaining to several aspects of damage tolerant aircraft structure.

- 1) Regarding analysis methodology, initial flaw locations and the requirements of MIL-A-83444, the following are recommended:
 - New analysis methodology is needed to account for details of the fastener system that enhance the damage tolerance of the joint, such as clamp-up, fastener interference, and faying surface friction (without sealant). The criteria in MIL-A-83444 need to be flexible enough to reward the use of damage tolerant fastener systems, provided that the damage tolerance improvements are demonstrated by test, that the life extending parameters in the fastening system are identified, and that adequate quality control is present in the manufacturing line to assure that the necessary level of these parameters is maintained. For joints with these damage tolerant systems, the assumption of 0.005-inch continuing damage flaws at all holes, used now as an analysis expedient, should not necessarily be required.

- The continuing damage site located in the same hole as the primary 0.050-in. crack, but diametrically opposite, was found to be the most critical location for continuing damage. Hence, revisions to MIL-A-83444 should be made to include this most critical continuing damage location whenever initial continuing damage flaws are assumed in damage tolerance analysis.
 - For damage tolerance testing as well as analysis, the initial corner flaws must be located at whichever surface the initial growth rate will be a maximum. Neglecting the effect of environment (which will accelerate crack growth at an exposed surface) the maximum growth rate occurs where the cyclic tensile stresses are maximum. The cyclic tensile stresses are maximum at the faying surfaces of high-load-transfer joints. At low-load-transfer fasteners they may be at either surface depending upon the relative magnitudes of plate bending and fastener load transfer.
 - The most critical initial flaw in the stringer-reinforced specimens with two rows of fasteners was the crack that grew away from the influence of the stiffener. Initial flaws located near a free edge of a member also tend to grow rapidly, both as they approach the edge and after breaking through the edge to form an edge notch or edge crack. These are recommended for consideration as the most critical locations for initial flaws in damage tolerance analyses and tests.
 - For fail-safe structure the critical location for damage initiation in the remaining structure is usually at a fastener hole just outside the plane of cracking of the damaged neighboring member, where the load transfer of the fastener is a maximum. These sites should be monitored for crack initiation in damage tolerance tests, and 0.005-in. remaining structure damage flaws, if assumed in analysis, should be assumed at these locations.
- 2) For damage tolerance testing the following guidelines are recommended:
- To whatever extent is appropriate, the specimen preparation and precracking procedures of this program should be utilized. However, 0.005-inch initial continuing damage flaws should not be intentionally introduced, neither with a razorblade nor by any other means. These continuing damage flaws are presently required by MIL-A-83444 as an analysis expedient only and were not intended to be intentionally introduced into damage tolerance test specimens.
 - The structure should be subjected to spectrum fatigue loading, using, when feasible, a somewhat simplified, repetitive loading spectrum that will mark the fracture surface for easy interpretation, yet will be sufficiently representative of anticipated service loadings. The once per lifetime maximum load and other extremely infrequent peak loadings cannot be relied upon to always occur in service. Thus, they should be excluded, in order not to introduce their beneficial retardation effects into a worst-case test.

- The specimen should have sufficient size and lateral supports to represent the overall structural stiffness and deflections as they affect crack growth for all applied loadings and anticipated damage conditions. Strain gages and deflection measurements should be used intermittently during testing to verify that the specimen is responding as anticipated.
 - When feasible, representative environment and loading frequencies should be used.
 - A crack growth analysis of the test should precede the testing. This can aid in data gathering while increasing the confidence levels of both the analytical and the experimental result.
- 3) To better take advantage of the crack arrestment characteristics of Hi-lok fasteners with full torque the following are recommended:
- Improvements to the fatigue design of the Hi-lok collar to minimize cracking should be considered. When the collar cracks it is less effective in crack arrestment.
 - When appropriate in the repair of damaged structure or damage tolerance test specimens, the fully-torqued Hi-lok fastener should be installed in a stop-drill hole. The superiority of this procedure over simple stop-drilling was amply demonstrated in this program.
 - Improved analysis methods need to be developed to quantitatively account for fastener torque.
- 4) The testing in this program was conducted on a limited set of structural specimens loaded primarily in constant amplitude uniaxial cyclic tension. The emphasis was on slow stable flaw growth rates related to the slow crack growth requirements of MIL-A-83444 for newly-designed damage tolerant mechanically-fastened structure. The design, maintenance and verification of damage tolerant metallic aircraft structure could be greatly enhanced by further investigations involving other structural configurations, fastening system parameters, loading and environmental conditions, and damage conditions, or by work which emphasizes the residual strength requirements of MIL-A-83444 for complex damaged structure.

REFERENCES

1. "Airplane Damage Tolerance Design Requirements," MIL-A-83444 (USAF), Military Specification, United States Air Force, May 1974.
2. Brussat, T. R., "Fatigue Crack Growth, Arrest and Reinitiation Along a Row of Holes," LR 26806, Lockheed-California Company, December 1974.
3. Jarfahl, L. E., "Optimum Design of Joints: The Stress Severity Factor Concept," Fifth ICAF Symposium, Melbourne, Australia, May 1967.
4. Chiu, S. T. and Brussat, T. R., "Summary of 1976 Independent Research in Fracture Mechanics Analysis Methods," LR 27703, Lockheed-California Company, December 1976.
5. Young, L. and Brussat, T. R., "Summary of 1975 Independent Research in Fatigue and Fracture Mechanics Methods," LR 27298, Lockheed-California Company, December 1975.
6. Walker, E. K., "The Effect of Stress Ratio During Crack Propagation and Fatigue for 2024-T3 and 7075-T6 Aluminum," Effects of Environment and Complex Load History on Fatigue Life, ASTM STP 462, January 1970.